GEORGIA DOT RESEARCH PROJECT 14-35

FINAL REPORT

EXTENDING HYRISK TO PREDICT SCOUR RISK AS A FUNCTION OF SOIL ERODIBILITY CHARACTERISTICS

OFFICE OF RESEARCH
15 Kennedy Drive
Forest Park, GA

1.Report No.: FHWA-GA-RPXX	2. Government Accession No.:	3. Recipient's Catalog No.:

4. Title and Subtitle: Extending HYRISK to predict scour risk as a function of soil erodibility characteristics	5. Report Date: February, 2016
	6. Performing Organization Code:
7. Author(s): Laurie A. Garrow, Terry W. Sturm, P.E., Emma Bones	8. Performing Organ. Report No.:
9. Performing Organization Name and Address: Georgia Institute of Technology, 790 Atlantic Drive, Atlanta, GA 30332-0355	10. Work Unit No.:
	11. Contract or Grant No.: GDOT 14-35
12. Sponsoring Agency Name and Address: Georgia Department of Transportation, Office of Research, 15 Kennedy Drive, Forest Park, GA 30297-2534	13. Type of Report and Period Covered: Final; May 2014 – December 2015
	14. Sponsoring Agency Code:

15. Supplementary Notes:
Prepared in cooperation with the U.S. Department of Transportation, Federal Highway Administration.

16. Abstract:
The majority of bridge failures in the U.S. are the result of bridge foundation scour. However, determining which bridges are most vulnerable to scour is challenging – particularly in Georgia where more than 5,000 bridges have unknown foundations. This project develops an approach that associates the critical shear stress of a soil to its USCS soil group classification. This approach is applied to approximately 40 bridges in Georgia using HYRISK, a scour risk assessment tool, and shows how incorporating soil property information changes the expected financial losses associated with a bridge failure. This is important, as it enables engineers to use soil property information that is commonly found on boring logs to direct limited maintenance funds to those bridges that are most at risk to scour failure.

17. Key Words: bridge scour, risk assessment, soil erodibility, critical shear stress	18. Distribution Statement:		
19. Security Classification (of this report): Unclassified	20. Security Classification (of this page): Unclassified	21. Number of Pages: 92	22. Price:

GDOT Research Project No. 14-35

Final Report

EXTENDING HYRISK TO PREDICT SCOUR RISK AS A FUNCTION OF SOIL ERODIBILITY CATEGORIES

By
Laurie A. Garrow
Associate Professor

and

Terry W. Sturm
Full Professor

and

Emma Bones
M.S. Student

Georgia Institute of Technology

Contract with

Georgia Department of Transportation

In cooperation with

U.S. Department of Transportation
Federal Highway Administration

February, 2016

TABLE OF CONTENTS

LIST OF TABLES

Table Page

LIST OF FIGURES

Figure Page

NOMENCLATURE

Bridge scour: the removal of sediment and soil and the weathering of rock from around bridge abutments and piers. Scour can be viewed as a subset of erosion processes that specifically occurs around bridge piers and abutments.

Clay Fraction (CF): the active, binder fraction of fine-grained soils composed of clay minerals that are conventionally assumed to be constituted by particles <2 μm in size and distinguished by their plasticity and platy structure having strong interparticle forces.

Critical shear stress (CSS): the hydrodynamic force per unit surface applied in the streamwise direction of water flow over soil that is necessary to overcome resisting forces and initiate particle movement, or erosion.

Critical velocity: the velocity of water flow over soil that is necessary to initiate particle movement. However, this is not as unique a measure of incipient motion as critical shear stress because critical velocity is dependent upon water depth.

Erodibility Class: classification of the resistance of a soil to erosion or scour based on its critical shear stress. There are four classes identified in this report: very erodible, erodible, moderately resistant, and resistant. The term class will always refer to the erodibility category.

Liquid Limit (w_{LL}): the water content at which a soil changes from plastic to liquid states.

Plastic Limit (w_{PL}): the water content at which a soil changes from a semisolid to a plastic state.

Plasticity Index (I_p): measure of the plasticity of a soil, or ability to be deformed while maintaining its shape. Plasticity index is the difference between the liquid limit and the plastic limit ($I_p = w_{LL} - w_{PL}$).

Shields' Parameter: the nondimensional variable used to determine the initiation of particle movement in a fluid flow caused by shear forces on the soil. It represents the ratio of shear forces initiating erosion to gravitational forces resisting erosion.

Soil Category: the term that distinguishes between the two main soil categories: fine-grained soils and coarse-grained soils. The term category will always refer to this broad separation of soils.

Soil Type: the more specific term that separates the larger soil categories into smaller divisions. These include the soil types seen on the plasticity chart (i.e. CL, CH, ML, etc.) and the coarse-grained division of soil types (i.e. GW, SP, SW, etc.). Type with always refer to these more specific categories.

Water content: the ratio of the weight of water to the weight of the solids in a soil sample.

LIST OF SYMBOLS OR ABBREVIATIONS

A	Activity
a	Erosion rate constant
CSF	Clay-size fraction in a soil sample defined as the fraction by weight smaller than 2 μm
CSF^{Pred}	Predicted clay size fraction of the soil
d_*	Dimensionless particle diameter
d_{50}	Median particle diameter
E	Mass rate of erosion per unit surface area
E_c	Critical rate of erosion per unit surface area
$Fines$	Percent of fines (silt+clay) in a soil sample
I_p	Plasticity index
K_2	Soil risk adjustment factor
M	Erosion rate constant
n	Number of observations in a dataset
ρ_{dry}	Dry density of soil
R^2	Coefficient of determination
$Adj\ R^2$	Coefficient of determination adjusted for multiple predicting variables
S	Channel slope
τ	Bed shear stress
τ_c	Critical bed shear stress initiating erosion
τ_{*c}	Shields' Parameter

w	Water content
w_{LL}	Liquid limit
w_{PL}	Plastic limit
$\Delta y/\Delta t$	Best-fit slope of the piston displacement as a function of time
γ	Specific weight of water
γ_s	Specific weight of soil
y	Flow depth

EXECUTIVE SUMMARY

As scouring around foundations is the most common cause of bridge failures, one of the most pressing questions of this research is to determine whether or not it is possible to predict the critical shear stress of different soil types using only soil property information. This report shows that it is possible to predict critical shear stress and determines the soil properties that are required to predict the critical shear stress based on soils from Georgia. Multiple methods to predict soil erodibility categories are developed based on the amount of soil information available to the researcher. The report shows how the methods to predict soil erodibility can be integrated with HYRISK, a scour risk assessment tool. In particular, the probabilities of bridge failures and expected economic losses are calculated for approximately 40 bridges in Georgia; soil erodibility characteristics for these bridges are calculated using the methods developed in this report. The goal of this report is to provide a faster and more cost-effective approach to calculate critical shear stress ranges likely to be encountered at a bridge foundation. Implementation of theses methodologies will help balance funding for new and existing bridges while simultaneously ensuring safe bridge foundation and minimizing economic consequences associated with overbuilding a bridge and/or having to retrofit or replace a bridge that has scour damage due to underbuilding it to withstand a major storm event.

CHAPTER 1

INTRODUCTION

On April 5, 1987, the Schoharie Creek Bridge collapsed in New York State, killing ten people. The failure, that was attributed to scour around the bridge piers, launched a new research area in bridge design and maintenance focusing on scour and the physical processes associated with bridge scour.

Background

Scouring around foundations is the most common cause of bridge failures (Arneson et al., 2012). In 1994 and 2009, the state of Georgia experienced record-breaking flooding in excess of the 500-year storm event in several counties. In the 1994 floods, 43 (27%) of Georgia's 159 counties were declared federal disaster areas, including counties in metro Atlanta (CDC, 1994). During the 2009 floods, five counties in the metro Atlanta area (Fulton, Gwinnett, Cobb, Douglas, and Carroll) experienced floods in the 0.2 percentile (or equivalent to a 500-year storm) (Gotvald et al., 2010). During the 1994 floods, the increased flow scoured foundations and compromised infrastructure, causing the total failure of 31 state-owned bridges and requiring repairs to over 200 bridges. Additionally, the 1994 floods caused the deaths of 28 people, and the 2009 floods resulted in the deaths of eight people (CDC, 1994; Cook et al., 2009). In 1994, the damage caused by flooding to the Georgia Department of Transportation's (GDOT's) infrastructure system was $130 million, and in 2009, total damages from flooding were $193 million (Arneson et al., 2012; Gotvald et al., 2010). Due to the intensity of recent floods in Georgia (as well as other

states) and the high cost in lives and resources, identifying those bridges that are most at risk to fail due to scour and ensuring future bridge design guidelines properly account for increased intensity and frequency of rainfall events have arisen as major areas of research.

Many researchers are concerned that bridges that recently survived an *N*-year storm event may not withstand another major storm. This concern is driven by growing evidence that the increased intensity of flooding events seen in Georgia will continue and may even increase in coming years across the entire U.S. This is especially concerning for bridges that were built using precipitation and flood stage measurements fifty years ago which do not represent the increased intensity of flooding events that are predicted in the future. This shift towards more intense rainfall and flooding events indicates that the current design models may not be sufficiently robust to predict and design for future conditions (Milley, et al., 2008 as reported in NRC, 2009). Therefore, many researchers have called for new design standards that are strong enough to ensure bridge reliability during more intense and frequent weather events (IPCC, 2007; U.S. DOT, 2006 as referenced in Schmidt, 2008). To develop stronger design standards, researchers need to better understand the hydrodynamics of the scour process and the erosion resistance of soils at bridge foundations. An improved understanding of how scour occurs – and under what conditions – will allow researchers to develop more robust bridge design standards for *future* construction. Moreover, if researchers could associate scour with soil properties that are routinely recorded on boring logs, they could better assess scour failure risks associated with *existing* bridge infrastructure.

Two factors that are important to consider in bridge design and maintenance are time and money. In an era where funds for infrastructure construction, maintenance, and improvements are becoming scarcer, it is critical for agencies to prioritize expenditures on activities to help minimize the lifetime risk of bridge failures and associated economic impacts. However, there are often trade-offs that must be made between the initial amount of money spent to build a bridge and the subsequent amount of money that is required to repair or replace a bridge that has been compromised or failed due to scour. The HEC-18 circular states that in 1994 over 500 bridges in the U.S. were damaged during the floods, and of those bridges, over 250 needed to be repaired or replaced (Arneson et al., 2012). As noted earlier, within Georgia, the costs of replacing and repairing over 200 bridges that were damaged in 1994 cost $130 million (Arneson et al., 2012). Fifteen years later, the 2009 floods caused over $193 million in total damages (Gotvald et al., 2010). Some of these repair and replacement costs potentially could have been avoided by initially building these bridges to higher design standards; however, with limited resources, this likely would have resulted in fewer bridges being constructed. A transportation network with fewer bridges can result in higher transportation costs, which can impede economic activity. Therefore, an important goal of bridge design becomes balancing: 1) the costs incurred at the beginning of a project to ensure that probability of failure due to scour is minimized across the portfolio of bridges in a region; with, 2) potential costs that may be incurred in the future if one or more bridges do indeed fail. Balancing these objectives should consider short-term and long-term economic impacts.

Some state DOTs, including GDOT, currently balance these conflicting objectives by using conservative assumptions regarding the erodibility of soils that are uniformly applied to all new bridge designs. The depth of a scour hole around a foundation is determined by the complex interaction of the water moving over the soil surrounding the foundation. Although this interaction is not fully understood, the two main components that affect the scour depth are the river hydrodynamics and properties of the soil at the bridge pier and abutment foundations. Currently, GDOT assumes a median grain diameter based on the sands normally used by the Federal Highway Administration (ranging from very fine sand to very coarse sand). No fine-grained soils are considered and soil erodibility is not related to the separate categories of coarse-grained soils (Sturm et al., 2008). Therefore, the depth of the foundation is determined primarily based on the hydraulic calculations of the flow properties associated with the bridge obstruction and constriction and not on the geotechnical analysis of the soil. However, it has been shown that different soils can be more or less resistant to erosion and can fall into various erodibility categories (very erodible, erodible, moderately resistant, resistant, and very resistant) (Hanson and Simon, 2001; Thoman and Niezgoda, 2008). This is important, as the more resistant a soil is to scour, the smaller the final scour hole depth. Thus, by using soil information, engineers can potentially apply less conservative assumptions for a subset of new bridge designs and reallocate limited resources that would have been spent on "overbuilding" this subset of bridges to other bridges that are most susceptible to scouring and would benefit from more conservative design assumptions.

Information about soil properties can also support better allocation of funding for repair activities on existing bridges. To help determine which existing bridges are most vulnerable to scour, FHWA developed a risk-assessment tool called HYRISK. HYRISK can be used to calculate the probabilities of bridge failures due to scour and can then be used to rank bridges and identify those with high scour failure risks and economic losses. However, one of the key limitations of HYRISK is that it does not incorporate risk adjustment factors for soil factors associated with erodibility. Information about soils is clearly one of the most important factors influencing scour; however, soil factors associated with soil erodibility were not included in the original version of HYRISK developed by the FHWA. This is because the original HYRISK model was built exclusively from data inputs available in the National Bridge Inventory (NBI) database; information about soils is maintained in state – not national – databases and thus was excluded from FHWA's original HYRISK model.

To incorporate information about soil properties into bridge design, maintenance, and monitoring activities, the critical shear stress of a soil would need to be determined to analyze how resistant a particular soil is to scour. Ideally, this would be accomplished by testing a boring sample from the pier and abutment locations in a hydraulics lab to measure the critical shear stress. This lab-measured critical shear stress would then be incorporated into the hydraulic analysis to find a more accurate prediction of the scour depth. Unfortunately, this is a lengthy and expensive process that cannot be done for every bridge. Despite this obstacle, experiments can be applied to various soil types to determine which properties affect the erodibility of soils. Ideally, these properties would be easy to

determine or would be shared among soil types, allowing engineers to determine the erodibility of soil based purely on one or two soil properties. This report focuses on several key methods to predict the critical shear stress of soils that do not involve returning a boring sample to a lab for critical shear stress tests. The goal of these methodologies is to provide a faster and more cost-effective approach to calculate critical shear stress ranges likely to be encountered at a bridge foundation. Implementation of these methodologies will help balance funding for new and existing bridges while simultaneously ensuring safe bridge foundations and minimizing economic consequences associated with overbuilding a bridge and/or having to retrofit or replace a bridge that has scour damage due to underbuilding it to withstand a major storm event.

Research Questions

Based on the difficulties associated with measuring the critical shear stress of a soil via a lab test, one of the most pressing questions of this research is to determine whether or not it is possible to predict, to a high degree of certainty, the critical shear stress of a wide range of soils from Georgia using only soil property information. If it is possible to accurately predict critical shear stress, it must be established how many soil properties are required to accurately predict the critical shear stress. Also if not all of those properties are available, it must be determined if it is still possible to predict the critical shear stress and how much the lack of availability of certain soil properties may affect the accuracy of the predicted soil erodibility classifications. Finally, there is the potential for a more effective method to be developed and implemented for bridge maintenance; incorporating knowledge about the critical shear stress of soils surrounding a bridge foundation, this

method will result in time and cost savings in addition to safety improvements over the life of a bridge.

Major Contributions

This work contributes to the literature by developing a methodology to predict critical shear stress as a function of soil erodibility properties. A second major contribution of this study is that it uses the methodology above to extend HYRISK to include a risk adjustment factor that accounts for soil erodibility. This is important, as the adjustment factor will enable GDOT (and potentially other state DOTs) to calculate scour risks and associated economic losses for existing bridges as a function of soil types which are indicative of their erodibility or scour susceptibility. The results can be implemented by GDOT and used to prioritize the selection of bridges for Phase I scour screenings. Given the limited resources to conduct these screenings, it is critical that the bridges selected for screening are the ones that exhibit the highest risk of scour failures.

Throughout this report, uncertainties associated with determining the critical shear stress of soils will be discussed. Each technique developed to measure a soil's critical shear stress has an associated level of prediction error, and each equation or method proposed to predict critical shear stress of soils has an associated range in which this prediction error is minimized. This report builds on the research presented by several other researchers that utilizes the concept of erodibility categories to divide ranges of critical shear stresses into specific classes: very erodible, erodible, moderately resistant, resistant, and very resistant (Thoman and Niezgoda, 2008; Hanson and Simon, 2001). These erodibility categories

allow for uncertainty when predicting critical shear stress. Additionally, these classes can be easily translated into a HYRISK parameter.

By using the methodologies described in this report, engineers can more effectively utilize resources to design bridges that are safe and are better suited to the soil properties at their locations. Additionally, engineers can use the erodibility categories to create a new ranking of bridges most at risk to scour failures, enabling a more efficient use of funds for operation and maintenance of bridges across Georgia.

Outline

This report is organized into several chapters. Chapter 2 presents a literature review that explains the different geotechnical soil classification systems (USCS, ASTM, AASHTO, and British Standard) and the methodology each system uses to divide soils into different types. None of the classification systems were specifically designed for determining the critical shear stress of soils. Thus, each system has advantages and disadvantages with respect to its use in predicting the critical shear stress of soils. The prediction accuracy obtained solely from soil type information could be poor for certain soil types and is investigated in this report. To build upon the understanding of critical shear stress, the literature review then examines the various methods researchers have used to measure and analyze the critical shear stress of soils. Additionally, the uncertainty associated with each method to measure critical shear stress of soils is also explored. Two main categories of measuring critical shear stress exist, in-situ techniques and laboratory techniques. In-situ techniques include submerged impinging jets, benthic flumes, turbulent motion created above the bed with propellers or oscillating horizontal grids, and streams

of water generated with bell-shaped funnels above the bed. Laboratory techniques involve the extrusion of a soil sample in open or enclosed flumes. Finally, the development and use of HYRISK as a risk assessment tool for bridge failures due to scour is explained so that it can be expanded upon later in the report.

Chapter 3 explains the methodology developed to predict the critical shear stress of a soil sample using varying amounts of information about the soil. Chapter 4 used the methodology developed in Chapter 3 to predict the erodibility categories for soil samples from bridges across Georgia. These erodibility categories are used to develop a set of risk adjustment factors that are integrated into HYRISK. Bridge failure probabilities and associated expected economic consequences calculated from the "existing" and "enhanced" versions of HYRISK are compared and demonstrate how knowledge of soil erodibility affect the relative ranking of bridges in Georgia. The report concludes with a summary of major findings and directions for future research.

CHAPTER 2

LITERATURE REVIEW

This chapter presents a literature review that contains five sections. The first section, which introduces vocabulary and fundamental soils information needed to comprehend the report, covers four different geotechnical soil classification systems and describes how each system divides soils into different types. The second section provides an overview of methods used to measure and analyze the critical shear stress of soils; a particular emphasis is placed on discussing the prediction accuracy associated with each method. The third section covers one particular method in detail, namely the open flume laboratory experiments conducted by the Georgia Tech research team of Navarro, Hobson, and Wang under the direction of Dr. Terry Sturm. Initially, Navarro (2004) developed an equation to predict the critical shear stress of soil samples that were collected in the field. Hobson (2008) later refined Navarro's equation through the use of additional soil samples, and this refined equation is referred to as the Navarro/Hobson equation (Hobson et al., 2010). Wang (2013) developed an equation that predicts the critical shear stress of fine-grained soil samples. The fourth section, which represents one of the major contributions of this study, presents a conceptual framework for grouping ranges of soil critical shear stresses into a broad set of erodibility categories that account for uncertainty in measurements and predictions. Finally, the fifth section provides an overview of the development and use of HYRISK as a risk assessment tool for bridge failures due to scour. The erodibility categories introduced in Section 4 will be used to create a set of risk

adjustment factors for HYRISK that predict bridge failures as a function of (simple) soil properties available through boring logs.

Soils Background

On the most basic level, soils are grouped according to texture into four main types: clay, silt, sand, and gravel. Sand and gravels compose coarse-grained soils whereas clays and silts form the fine-grained category (Budhu, 2011). When comparing coarse and fine grained soils, coarse-grained soils will feel gritty and rough whereas fine-grained soils will feel smooth when rubbed between an individual's fingers. These different textures are due to differences in median grain sizes and particle size distributions (Budhu, 2011). For this reason, the division between coarse and fine grained soils occurs at a specific median particle diameter. However, this division differs depending on which system is being used to describe the soil types.

Over the years, four main soil classification systems have been developed to describe the division between fine and coarse grained soils. The four main systems are: the Unified Soil Classification System (USCS), the American Society for Testing and Materials (ASTM), which is modified from the USCS system, the American Association of State Highway and Transportation Officials (AASHTO), and the British Standards (BS). The USCS system and ASTM system are nearly identical and use the same symbols to describe soil types. However, the ASTM system was developed to provide a better schema to classify mixed soils (Budhu, 2011). The AASHTO system is used to determine the suitability of soils for earthworks, embankments, and road-bed materials (Budhu, 2011). The British Standards system is not used in the U.S., and therefore, will not be reviewed in

this report. Although there are extensive flow charts for how to best separate soils into various types, the fastest method is to separate soils based on median grain size.

Due to the similarities between the USCS and ASTM and the fact that GDOT uses the USCS system for their boring logs, the USCS will be used exclusively in this report. The USCS system describes both the texture and grain size of soils. The first letter of the classification system divides the soil by grain size into gravel, sand, silt, clay, and organic with corresponding letters of G, S, M, C, and O. The second letter of the classification system divides the soil based on texture. Coarse-grained soil can be either poorly graded (uniform particle sizes) or well graded (diverse particle sizes) with corresponding letters of P or W. Fine-grained soils can either have high or low plasticity depending on its deformation properties and are denoted with corresponding letters of H or L. Tables 2.1 and 2.2 provide additional information on the criteria used to define the first and second letters of the USCS system.

Table 2.1: First letter of the USCS system (Holtz and Kovacs, 1981).

Letter	Definition	Size
G	Gravel	> 50% of soil retained on No. 4 (4.75 mm) sieve
S	Sand	≥ 50% of soil passes No. 4 sieve (4.75 mm)
M	Silt	> 50% of soil passes No. 200 (0.075 mm) sieve
C	Clay	> 50% of soil passes No. 200 sieve (0.075 mm)
O	Organic	N/A

**Note: The USCS system does not differentiate between silt and clay on a size basis but rather uses Atterberg limits.

Table 2.2: Second letter of the USCS system (Holtz and Kovacs, 1981).

Letter	Definition
P	Poorly graded
W	Well graded
H	High plasticity ($w_{LL} > 50$)
L	Low plasticity ($w_{LL} < 50$)

Fine-grained soils are often displayed on a plasticity chart, and certain soils fall into specific regions of the chart. The plasticity chart is the most widely accepted method to classify fine-grained soils, and it was created by plotting experimental results from soils tested from around the world on a figure including liquid limit and plasticity index, as shown in Figure 2.1 (Budhu, 2011). Some common soil types are high plasticity clay (CH), low plasticity clay (CL), high plasticity silt (MH), low plasticity silt (ML), high plasticity organic soil (OH), and low plasticity organic soil (OL). Figure 2.1 portrays an example of a plasticity chart and shows how each soil type is classified according to its plasticity index, I_p, defined as I_p = *Liquid Limit – Plastic Limit*, where the liquid limit, $w_{LL,}$ is determined using the Casagrande cup method, and the plastic limit, w_{PL}, is found by rolling the soil into a thread until it breaks (ASTM International, 2005). The "A" line separates plastic from nonplastic soils. Therefore, clay, which is plastic, is separate from silt and inorganic soils, which are not plastic. The "U" line is the dashed line above the "A" line, and no soils should plot above the "U" line which represents the plasticity index limit of natural soils.

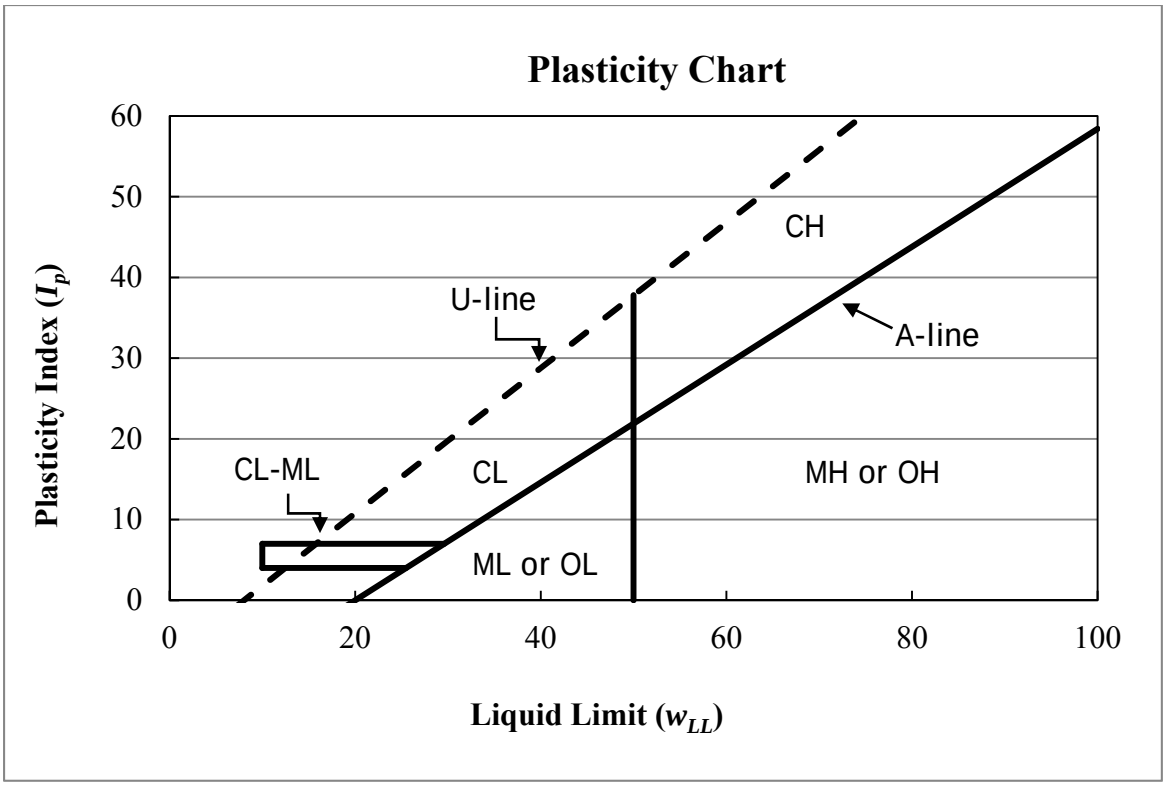

Figure 2.1: Plasticity chart of USCS system (ASTM International, 2011a).

The plasticity chart is plotted using measured values of liquid limit and plasticity index for each fine-grained soil. The problem with this approach for our particular research question is that neither the liquid limit nor the plasticity index is provided in boring logs.

Techniques to Measure Critical Shear Stress

To use certain soil properties as predictors of soil critical shear stress, many techniques have been developed to measure critical shear stress in both laboratory and in-situ situations. Hobson (2008) provides a thorough literature review of many of the techniques as well as an assessment of their advantages and disadvantages. This literature review builds upon Hobson's review by assessing uncertainties with the critical shear stress

measurements that may arise when using a particular technique; therefore, a summary of each technique along with disadvantages, advantages, and sources of error for each method will be provided. A distinction is made between those methods that are conducted in-situ and those that are completed in a laboratory after sampling soils. Houwing and van Rijn (1998) and Hanson and Cook (2004) both argue that in-situ tests are preferred because disturbances caused by moving and storing of soil samples could lead to higher measured critical shear stresses than in natural conditions. However, laboratory tests provide a larger amount of control over the experiment as it progresses. Due to the trade-offs between in-situ and laboratory tests, an assessment of each type of test will be made separately. Table 2.3 compares the advantages and disadvantages of each method while Tables 2.4 to 2.9 show the researchers who have contributed to each method of determining the critical shear stress of a soil. Definitions for each method are provided below:

In-situ Techniques

- *Submerged Impinging Jet*: A nozzle is submerged in water directed towards the bed of a river, stream, or lake. A jet of water issues from a nozzle placed at the bed to measure the erosion rate, which is the depth of scour per unit time. The erosion rate is related to the jet velocity, a time function, and a soil parameter (Hanson, 1991).
- *Benthic Flumes*: Portable flumes that can be placed on the bed of a river, stream, or lake to measure the erosion rate of undisturbed bed sediments. Several types of flumes exist including the annular or race-way recirculating type or a straight, flow-through type. Both subaerial (flumes exposed to the atmosphere) and submerged

flumes are used, and water is pumped through the flume until erosion occurs (Tolhurst et al., 2009).

- *Turbulent Motion above Bed Generated by a Propeller*: A tube is lowered over the sediment sample to isolate it from the bed sediments. A propeller is then placed in the tube that generates turbulence and suspends sediments in the tube. These sediments are then pumped into a storage vessel to record total sediment suspension at the end of the experiment, and water is returned to the tube with the sediment (Schunemann and Kuhl, 1993).

- *Turbulent Motion above Bed by Oscillation of Horizontal Grid*: A portable tube is lowered over sediment to isolate it from the surrounding bed sediments. A horizontal grid oscillates vertically to create turbulence and causes resuspension of the sediments which can be measured to determine the erosion rate (Tsai and Lick, 1986).

- *Stream of water generated with bell-shaped funnel above bed*: A bell-shaped funnel is placed on the bed to isolate sediment from the rest of the bed. Water is then pumped up the center of the bell and replaced by water drawn down the sides of the bell that flows radially over the sediment from the sides of the bell towards the center, similar to a sink flow. Water pumped from the bell is retained in a reservoir where turbidity can be measured (Willamson and Ockenden, 1996).

Laboratory Methods

- *Open Flumes*: A basic three-boundary laboratory flume (two sides and bottom) through which water can be circulated to imitate the flow of a river or stream as open channel flow. A soil sample is then extruded into the flowing water to measure its erosion rate (Navarro, 2004; Hobson, 2008; Wang, 2013).
- *Enclosed Flumes*: A soil sample is extruded into a pipe with a rectangular cross section. Both the velocity of the water passing over the soil and the distance of the soil protrusion can be controlled (Briaud et al., 1999).

Table 2.3: Advantages and disadvantages of each technique for measuring critical shear stress (CSS).

Techniques	Method	Advantages	Disadvantages
In-Situ	Submerged Impinging Jet	1) Small and easy to handle (Houwing and van Rijn, 1998) 2) Repeatable results comparable to laboratory open flumes (Charonko, 2010)	1) Small test surface creates high variability based on bed irregularities (Houwing and van Rijn, 1998) 2) Shape and size of scour hole created by jet can affect shear stress measurements (Charonko, 2010) 3) Soil swell from entrained water can affect shear stress measurements (Charonko, 2010)
	Benthic Flumes	1) Need for logarithmic velocity profile can be avoided through use of stress probes or by measuring near-bed turbulence parameters (Aberle et al., 2003) 2) Fully takes into account the physical, chemical, and biological properties of a riverbed (Aberle et al., 2003)	1) Large size of instrument required to measure logarithmic velocity distribution (Houwing and van Rijn, 1998) 2) Boundary layer may not be fully developed in a flow-through flume (Aberle et al., 2003)
	Turbulent motion above bed generated by propeller	1) Small and easy to handle (Houwing and van Rijn, 1998)	1) Small test surface creates high variability based on bed irregularities (Houwing and van Rijn, 1998)
	Turbulent motion above bed by oscillation of horizontal grid	1) Small and easy to handle (Houwing and van Rijn, 1998)	1) Small test surface creates high variability based on bed irregularities (Houwing and van Rijn, 1998)
	Stream of water generated with bell-shaped funnel above bed	1) Small and easy to handle (Houwing and van Rijn, 1998)	1) Small test surface creates high variability based on bed irregularities (Houwing and van Rijn, 1998)

Table 2.3 (Continued): Advantages and disadvantages of each technique for measuring critical shear stress (CSS).

Techniques	Method	Advantages	Disadvantages
Laboratory	Open Flumes	1) Commonly used and results widely accepted (Charonko, 2010) 2) Tests have been performed for many decades and on a wide variety of soil samples (Charonko, 2010)	1) physical, chemical, and biological/microbiological sediment properties cannot be simulated accurately (Aberle et al., 2003)
	Enclosed Flume	1) Allows for control of pressure and turbulence intensity within flume (Briaud et al., 1999) 2) Sampling at the site via Shelby tubes allows for site-specific testing (Briaud et al., 1999)	1) physical, chemical, and biological/microbiological sediment properties cannot be simulated accurately (Aberle et al., 2003) 2) Limited volume of soil can be tested (Briaud et al., 1999)

Table 2.4: Comparison of Submerged Impinging Jet Techniques.

Researcher(s)	Year(s)	Uncertainty Parameter	Measurement/ Prediction Uncertainty	Published CSS Measurements	Soil/Flow Properties Measured	Soil Prop. used in Model	Soil Specific Model	Location
Paterson	1989	Critical Velocity, U_c	Measurement	No	Grain size dist., water content, salinity, diatom numbers, sediment water content	No model created	Cohesive	Marine
Allen et al.	1999	Erodibility coefficent, K	Prediction	No	Moisture content, wet and dry bulk density, void ratio, grain size dist., plasticity index	Activity, moisture content, wet and dry bulk density, void ratio, grain size distribution, plasticity index	No	Central Texas
Tolhurst et al.	1999	Critical eroding pressures, kPa	Prediction	Yes	Grain size dist.	Grain size	$d_{50} > 200$ µm	Not stated
Hanson and Simon	2001	Not Stated	N/A	Yes	critical shear stress, erodibility coefficient, erosion rate	No model created	50-80% Silt	Midwest, USA
Mazurek et al.	2001	Not Stated	N/A	Yes	Atterberg limits, activity, grain size dist., dry density	No model created	Cohesive	Lab Made
Potter et al.	2002	R^2, Jet Index	Prediction	Yes	Grain size dist., soil description, pH, conductivity, Atterberg limits, bulk density, water content	Grain size distribution, Atterberg limits	No	Central Mexico

Table 2.4 (Continued): Comparison of Submerged Impinging Jet Techniques.

Researcher(s)	Year(s)	Uncertainty Parameter	Measurement/ Prediction Uncertainty	Published CSS Meas.	Soil/Flow Properties Measured	Soil Properties used in Model	Soil Specific Model	Location
Ansari et al.	2003	Volume and depth of scour	Prediction	No	bulk density, grain size dist., organic carbon, Atterberg limits	No model created	No	Not stated
Watts et al.	2003	Critical shear stress	Measurement	Yes	Shear strength, critical shear stress, grain size dist., organic content, conductivity, wet and dry bulk density, water content, suspension index	No model created	Saltmarsh	Essex, UK
Wynn and Mostaghimi	2006	adjusted R^2, Critical Shear Stress	Prediction	Yes	Soil erodibility, CSS, aggregate stability, bulk density, specific gravity, water content, organic carbon, Atterberg limits, root length density, root volume ratio, pH, conductivity, K+, Mg2+, Ca2+, Na+, soil salt, potassium intensity factor, sodium adsorption ratio, grain size dist. (median grain size, % sand, % silt, % clay), water temperature, water conductivity, water pH, total suspended solids	Significantly different: soil erodibility, critical shear stress, bulk density, aggregate stability, organic carbon, grain size distribution, grain size standard deviation, plasticity index, soil pH, soil conductivity, potassium intensity factor	Plastic and Nonplastic equations	Blacksburg, VA

Table 2.4 (Continued): Comparison of Submerged Impinging Jet Techniques.

Researcher(s)	Year(s)	Uncertainty Parameter	Measurement/ Prediction Uncertainty	Published CSS Measurements	Soil/Flow Properties Measured	Soil Properties used in Model	Soil Specific Model	Location
Wynn et al.	2006	Critical shear stress, Pa	Measurement	Yes	Soil temperature, water content, air temperature, stream stage, freeze-thaw cycle, bulk density, precipitation	Soil temp., water content, air temperature, stream stage, freeze-thaw cycle, bulk density	No	Blacksburg, VA
Thoman and Niezgoda	2008	Not Stated	N/A	Yes	USCS name, critical shear stress, erodibility, Atterberg limits, water content, Dispersion ratio, Activity, % sand, % Silt, % clay, Specific gravity, Dry density, pH, Conductivity, Organic content, Cation exchange capacity, Soil adsorption ratio	Activity, Dispersion ratio, Specific gravity, pH, Water content	No	Wyoming
Thoman and Niezgoda	2008	Not Stated	N/A	Yes	USCS name, critical shear stress, erodibility, Atterberg limits, water content, Dispersion ratio, Activity, % sand, % Silt, % clay, Specific gravity, Dry density, pH, Conductivity, Organic content, Cation exchange capacity, Soil adsorption ratio	Activity, Dispersion ratio, Specific gravity, pH, Water content	No	Wyoming

Table 2.4 (Continued): Comparison of Submerged Impinging Jet Techniques.

Researcher(s)	Year(s)	Uncertainty Parameter	Measurement/ Prediction Uncertainty	Published CSS Measurements	Soil/Flow Properties Measured	Soil Properties used in Model	Soil Specific Model	Location
Mallison	2008	Not Stated	N/A	Yes	Bulk density, grain size distribution, specific gravity, Atterberg limits	Bulk density, grain size distribution, specific gravity, Atterberg limits	No	Many
Charonko	2010	Critical shear stress, Pa	Measurement	Yes	Grain size distribution, Atterberg limits, water content, bulk density	No model created	Cohesive	Many

Table 2.5: Comparison of Benthic Flume Techniques.

Researcher(s)	Year(s)	Uncertainty Parameter	Measurement/ Prediction Uncertainty	Published CSS Measurements	Soil/Flow Properties Measured	Soil Properties used in Model	Soil Specific Model	Location
Young	1977	Not Reported	N/A	No	Shear velocity, flume velocity	No model created	Marine	Not Reported
Gust and Morris	1989	Not Reported	N/A	No	Sediment concentrations, friction velocity	Sediment concentrations	Marine	Puget Sound
Amos et al.	1992a,b	Erosion rate, $kg/m^2/s$	Measurement	Yes	Grain size distribution, bulk density, water content, organic content, water temperature, salinity	Water depth	Marine	Bay of Fundy
Maa et al.	1993	Bed Shear Stress, Pa	Measurement	Yes	Grain size distribution, organic content, suspended matter	No model created	Marine	Chesapeake Bay and Middle Atlantic Bight
Ravens and Gschwend	1999	Critical shear stress, Pa	Measurement	Yes	Porosity, grain size distribution, organic content, erosion rate	No model created	Marine	Boston Harbor, MA
Aberle et al.	2002, 2003, 2004, 2006	Bed Shear Stress	Measurement	No	Bed shear stress, centerline velocity, wet bulk density, water content, organic content, and grain size distribution (median grain size, % sand, % silt, % clay)	Shear stress, critical shear stress, bulk density	No	Not Reported

Table 2.5 (Continued): Comparison of Benthic Flume Techniques.

Researcher(s)	Year(s)	Uncertainty Parameter	Measurement/ Prediction Uncertainty	Published CSS Measurements	Soil/Flow Properties Measured	Soil Properties used in Model	Soil Specific Model	Location
Debnath et al.	2007a,b	Erosion rate	Measurement	No	Grain size distribution, dry and wet bulk density, moisture content, loss on ignition, pH, conductivity	No model created	Cohesive	New Zealand
Ravens	2007	Bottom Stress	Prediction	No	Bulk density, total suspended solids, turbidity, flow rate, erosion rate	No model created	No	Wisconsin
Tolhurst et al.	2009	Not Reported	N/A	No	Literature Review	No model created	Muddy sediment	Not Reported

Table 2.6: Comparison of techniques involving motion above a bed generated by oscillation of a horizontal grid.

Researcher(s)	Year(s)	Uncertainty Parameter	Measurement/ Prediction Uncertainty	Published CSS Measurements	Soil/Flow Properties Measured	Soil Properties used in Model	Soil Specific Model	Location
Tsai and Lick	1986	Resuspended sediments, mg/L	Measurement	No	None Measured	No model created	No	Not Reported

Table 2.7: Comparison of techniques involving a stream of water generated with a bell-shaped funnel above the bed.

Researcher(s)	Year(s)	Uncertainty Parameter	Measurement/ Prediction Uncertainty	Published CSS Measurements	Soil/Flow Properties Measured	Soil Properties used in Model	Soil Specific Model	Location
Williamson and Ockenden	1996	log Shear stress, $\log_{10}\tau$	Measurement	Yes	Dry density, % sand, shear stress, range of shear stresses	No model created	No	Estuary

Table 2.8: Comparison of Open/Enclosed Flume Techniques.

Researcher(s)	Year(s)	Uncertainty Parameter	Measurement/ Prediction Uncertainty	Published CSS Measurements	Soil/Flow Properties Measured	Soil Properties used in Model	Soil Specific Model	Location
McNeil et al.	1996	Not Stated	N/A	No	Erosion rate, grain size distribution, organic carbon	No model created	No	Michigan Wisconsin
Roberts et al.	1998	Erosion rate	Measurement	Yes	Grain size, bulk density, shear stress, erosion rate	Graphical relationship for CSS as a function of grain size and bulk density	Noncohesive	Lab
Briaud et al.	1999, 2001	Not Reported	N/A	Yes	Unit weight, grain size distribution, water content, Atterberg limits, USCS, erosion rate	Model for scour depth based on initial erosion rate but no CSS model	No	Lab
Zreik et al.	1998	Not Stated	N/A	No	Erosional strength, mechanical strength, specific gravity, liquid limit, plastic limit	No model created	No	Boston blue clay
Ravisangar et al.	2001, 2005	R^2, Bed Shear Stress (Pa)	Prediction	Yes	Shear stress, flow rate, flow depth, median grain size, specific gravity, pH, BET surface area, conductivity, water content, zeta potential, rheological parameters	No model created	Georgia Kaolinite	Lab Made

Table 2.8 (Continued): Comparison of Open/Enclosed Flume Techniques.

Researcher(s)	Year(s)	Uncertainty Parameter	Measurement/ Prediction Uncertainty	Published CSS Meas.	Soil/Flow Properties Measured	Soil Properties used in Model	Soil Specific Model	Location
Ting et al.	2001	Not Stated	N/A	Yes	Atterberg limits, specific gravity, water content, grain size distribution, shear strength, CEC, SAR, pH, conductivity, unit weight, relative density	No model but inverse relationship of initial erosion rate & CSS noted	Porcelain clay and bentonite	Not Stated
Roberts et al.	2003	Not Reported	N/A	No	Suspended load, bedload, erosion rate	No model created	Noncohesive	Not Reported
Witt and Westrich	2003	Erosion rate	Measurement	No	Erosion rate, scour depth, bulk density	No model created	Cohesive	Germany
Navarro	2004	Shields' Parameter	Prediction	Yes	USCS name, Bulk density, Dry density, Water content, Organic matter content, Specific gravity, Void ratio, Porosity, Atterberg limits, Grain size dist. (median grain size, % sand, % silt, % clay)	Percent fines, median grain size	No	Georgia
Barry et al.	2006	Critical Shear Stress	Measurement	Yes	Dry and wet bulk density, grain size dist., clay type	No model created	Coarse	Lab Made
Krishnappan	2007	Not Stated	N/A	No	Bed shear stress, size dist. of sediment flocs, suspended concentration, erosion rate	No model created	Cohesive	Northwest Canada

Table 2.8 (Continued): Comparison of Open/Enclosed Flume Techniques.

Researcher(s)	Year(s)	Uncertainty Parameter	Measurement/ Prediction Uncertainty	Published CSS Measurements	Soil/Flow Properties Measured	Soil Properties used in Model	Soil Specific Model	Location
Ganaoui et al.	2007	Not Stated	N/A	Yes	Erosion rate, Stokes diameter, median Stokes diameter, particle Reynolds number	No model created	Marine and Fresh	Rhone River
Hobson	2008	Shields' Parameter	Prediction	Yes	USCS name, Bulk density, Dry density, Water content, Organic matter content, Specific gravity, Void ratio, Porosity, Atterberg limits, Grain size dist. (median grain size, % sand, % silt, % clay)	Percent fines, median grain size	No	Georgia
Wang	2013	Shields' Parameter	Prediction	Yes	Water content, dry and wet bulk density, grain size dist., Atterberg limits, specific gravity, specific surface, temperature, pH, conductivity	Water content, grain size distribution, dry and wet bulk density	Cohesive	Lab Made

Development of Equations to Estimate Critical Shear Stress

This section describes some of the most recent data collected in open flumes using Georgia soils. This research was conducted at Georgia Tech by Navarro (2004), Hobson (2008), and Wang (2013) under the guidance of Dr. Terry Sturm. The end products of the researchers' dissertations were equations that can predict the critical shear stress of soils based on a variety of physical properties. This section will explain how data was collected and measured by these researchers, and based on those measurements, how the equations were developed. Navarro completed his research in 2004, and Hobson conducted his research four years later using similar experimental techniques and combined his results with Navarro's. Therefore, the methods and results for Navarro and Hobson are combined in the following section.

Data Collection and Testing for Navarro and Hobson Data

The data used in this report comes from three researchers: Navarro, Hobson, and Wang. Navarro collected field soil samples in partnership with GDOT in 2004. Hobson later collected additional field soil samples in partnership with GDOT in 2008, choosing samples that would complement Navarro's samples. Soil collection sites were based on the seven main physiographic regions found in Georgia, and they were collected using Shelby tubes to extract soil from bridge foundations (Hobson, 2008). Where possible, several samples were collected from each region in order to ensure diversity in the soil samples. Figure 2.2 shows the location of each soil sample collected by Navarro and Hobson. Both the Southern Valley and Ridge and Southern Blue Ridge regions only have one sample,

and the Cumberland Plateau does not have any samples. However, the Cumberland Plateau is a very small and a minimally populated area of Georgia.

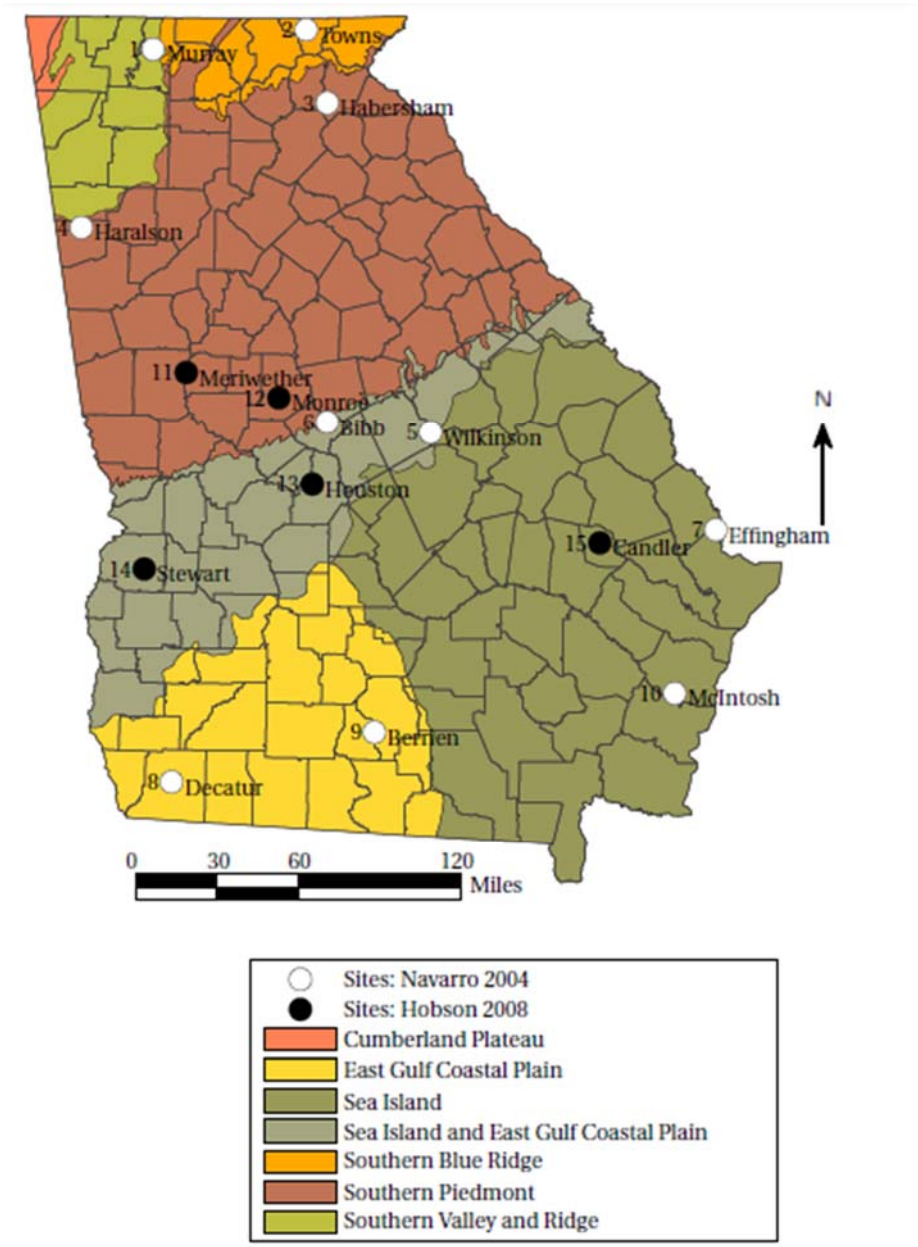

Figure 2.2: Sample locations for Navarro and Hobson and Georgia physiography (Alhadeff et al., 2000; Hobson, 2008).

In addition to geographic diversity, the samples were diverse in their physical properties, including mixtures of fine and coarse grained soils in varying percentages. Once the samples were collected, they were returned and stored in a constant-temperature room in the lab. Extensive geotechnical tests were then completed in order to determine important soil properties such as grain size distribution, bulk density, Atterberg limits, and organic matter content for each sample. To determine the critical shear stress of each Shelby tube sample, Hobson and Navarro inserted the sample into a piston that could be manually extruded or raised into a recirculating, rectangular, tilting flume. Figure 2.3 shows the experimental setup used by the researchers. The important parts to note in Figure 2.3 are the extruding piston which is used to push the Shelby tube sample into the flowing water, allowing it to erode due to the shear stress exerted by the flow. A cable-pull potentiometer is attached to the extruding piston in order to measure the distance that the piston has been raised.

During the testing by Navarro and Hobson, erosion occurred via two of the three modes identified by Mehta (1991). Pure surface erosion occurs when particles are eroded in a uniform fashion over the entire surface of the soil sample. Mass erosion happens when an entire section of soil fails due to a weak plane, and a large chunk of soil is eroded. Most soils experienced both modes of erosion, and the different modes are related to the amount of fines and the excess shear stress relative to the critical shear stress (Navarro, 2004). As mentioned above, the piston is manually extruded and therefore must be adjusted based on the erosion mode. However, the goal is for the soil sample to remain 1 mm above the fixed

gravel bed of the flume, and as the soil is eroded the researcher uses the piston to further extrude the soil, maintaining the 1 mm surface height (Hobson, 2008).

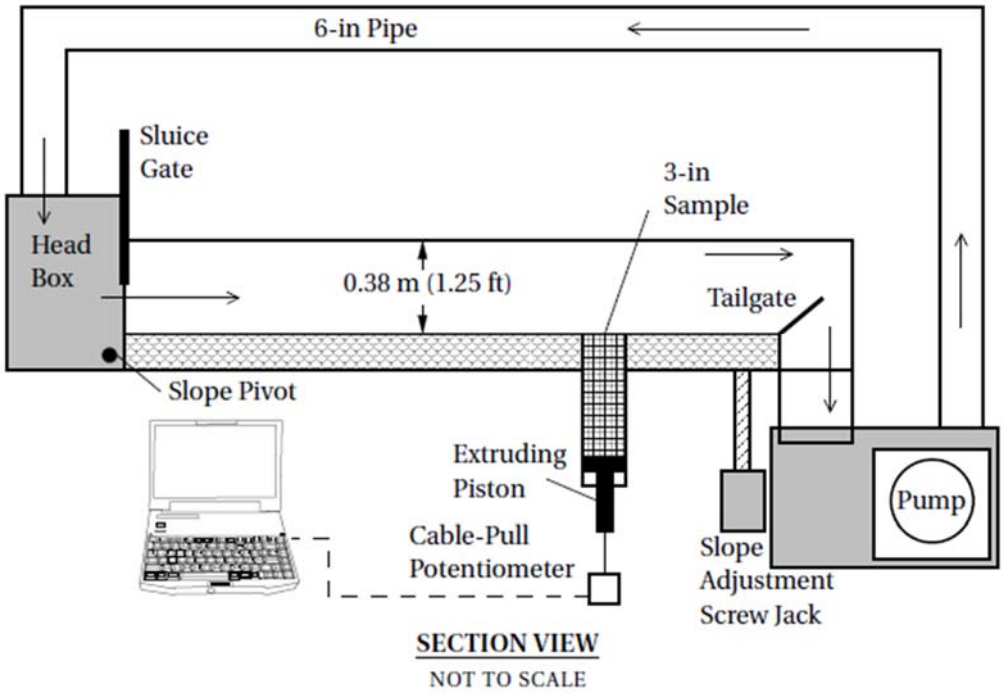

Figure 2.3: Section view of the tilting, recirculating flume Hobson (2008) and Navarro (2004) used for erosion testing. Source: Hobson (2008), Chapter 3 Figure 3.4.

To calculate the critical shear stress of each soil sample, Navarro (2004) and Hobson (2008) calculated the erosion rate using the following equation

$$E = \frac{\Delta y}{\Delta t}\rho_{dry} \tag{2.1}$$

where $\Delta y/\Delta t$ (typically measured as m/s) is the best-fit slope of the piston displacement data as the piston is manually raised over the course of the experiment, ρ_{dry} (typically measured as kg/m^3) is the dry density, and E (typically measured as kg/(m^2×s)) is the erosion rate per unit surface area. Once the erosion rate was determined for several values of bed shear stress, two models were used to find the critical shear stress as the intercept of the relationship between erosion rate and bed shear stress: the piecewise linear and exponential models. The piecewise linear model performed best when determining critical shear stress and estimating low erosion rates and the exponential model performed best when a model is required for the full range of shear stresses (Navarro, 2004). The following equations show the piecewise linear and exponential models that Navarro (2004) and Hobson (2008) used to find critical shear stress.

Piecewise Linear Model:

$$E = M \times \left(\frac{\tau - \tau_c}{\tau_c}\right) \tag{2.2}$$

where E is the erosion rate (kg/(m^2×s)), M is the erosion rate constant (kg/(m^2×s)), τ is the bed shear stress (Pa), and τ_c is the critical shear stress (Pa) at zero erosion rate.

Exponential Model:

$$E = E_c \times e^{a\left(\frac{\tau - \tau_c}{\tau_c}\right)} \tag{2.3}$$

where E is the erosion rate (kg/(m^2×s)), a is the erosion rate constant (unitless), τ is the bed shear stress, τ_c is the critical shear stress, and E_c is the critical erosion rate which Navarro (2004) determined to be 0.00190 kg/m^2/s as the value assigned to critical shear stress. Although boh methods were tried to measure the critical shear stress, all reported values in Navarro and Hobson used Eq. (2.2) as the best performing model.

The applied bed shear stress was determined from the uniform flow relationship as verified previously by direct measurement of the shear stress (Ravisangar et al. 2005):

$$\tau = \gamma y S \tag{2.4}$$

where γ is the water specific weight (N/m^3), y is the flow depth (m), and S is the channel slope (dimensionless). By using the above methodology and equations, Navarro and Hobson determined the critical shear stress for each soil sample. They converted the critical shear stress to a critical value of the dimensionless Shields parameter (Sturm 2010):

$$\tau_{*c} = \frac{\tau_c}{(\gamma_s - \gamma) d_{50}} \tag{2.5}$$

where τ_{*c} is the Shields parameter, τ_c is the critical shear stress, γ_s is the specific weight of the soil, γ is the specific weight of water, and d_{50} is the median grain size. Navarro (2004) used the original soil samples and the properties determined from those samples to perform a multiple linear regression analysis to find the properties that most affected the critical

Shields parameter. Based on Navarro's analysis, the following equation was proposed to estimate the critical Shields parameter.

$$\tau_{*c} = 0.586 \times 10^{2.67 \times Fines} \times d_*^{-0.337} \tag{2.6}$$

where τ_{*c} is the Shields parameter, *Fines* is the percent of fines in a soil sample in decimal form, and d_* is the nondimensional grain size. Hobson (2008) added more soil samples to Navarro's data, and based on the soil properties of the expanded dataset, Hobson also performed a linear regression analysis to augment the work done by Navarro. Based on the additional soil samples, Hobson was able to refine Navarro's original equation predicting critical values of the Shields parameter to the following form:

$$\tau_{*c} = 0.644 \times 10^{2.68 \times Fines} \times d_*^{-0.409} \tag{2.7}$$

where τ_{*c} is the Shields parameter, *Fines* is the percent of fines in a soil sample in decimal form, and d_* is the nondimensional grain size. Therefore, both Navarro and Hobson found that the Shields parameter could be best predicted by the percent of fines in the soil (including silt and clay) and the nondimensional particle size, d_*. Eq. (2.7) was used for all calculations throughout this report, and it will be referred to as the Navarro/Hobson (N/H) equation. Additionally, it should be noted that although Navarro and Hobson collected separate data and each had their own dataset, the final analysis included both Navarro and

Hobson's data. Therefore, the two datasets from each researcher will be referred to as one dataset in this report and called the Navarro/Hobson dataset.

Specimen Preparation and Testing for Wang Data

Based on the limited number of fine-grained soil samples collected by Navarro and Hobson, the next Georgia Tech researcher, Wang (2013), built upon their research by focusing only on fine-grained soils. Rather than collecting field samples, Wang (2013) mixed silt and clay size particles in the lab for flume tests. The specimens were prepared by mixing Georgia kaolin and ground silica in varying proportions by dry weight to create different samples for testing. It should be noted that Wang's samples were produced from fine-grained soils alone. Wang did not use sand or gravel in any of the mixtures. Water was added into the sediment mixture at a ratio of 160 ml of water to 100 g of sediments. After thoroughly mixing the sediment and water sample, the suspension was transferred to a Shelby tube where it was allowed to settle for approximately 24 hours. Once the sample was completely settled, the excess water was removed from the top of the soil sample. Sediment mixtures of 10%, 20%, 40%, 60%, and 100% kaolin by dry weight were tested by Wang.

To measure the critical shear stress of each soil sample, an extruding piston was placed into the bottom of the Shelby tube which was positioned in the flume bed with the top of the soil sample approximately level with the bed. The experiment setup was very similar to the setup used by Navarro (2004) and Hobson (2008) as shown previously in Figure 2.3. As the soil is eroded, the piston is manually raised into the flume to ensure that the exposed soil remains slightly above the fixed gravel bed of the flume. A cable-pull

potentiometer is used to record the height to which the sample is extruded by the piston, and this change in height versus time is recorded and entered into Eq. (2.1) to determine the erosion rate, E. Wang used Eq. (2.4) to find the bed shear stress, τ, and the following equation to determine the critical shear stress of a soil sample

$$E = M \times (\tau - \tau_c)^n \tag{2.8}$$

where E is the erosion rate, τ is the bed shear stress, and τ_c is the critical shear stress. To solve the equation for M, n, and τ_c, a nonlinear optimization problem was formulated and the unknown parameters were found using the Gauss-Newton algorithm. The objective function minimized errors between the observed values and those predicted by Eq. (2.8).

Once the critical shear stress of the soil sample has been determined, Eq. (2.5) can be used to find the Shields parameter for each soil sample. Additionally, Wang (2013) used conventional geotechnical tests to determine soil properties for the samples including water (moisture) content, dry and bulk densities, Atterberg limits, grain size distribution, specific gravity, and specific surface area. Wang used these properties and the Shields parameter of each soil sample to perform a multiple linear regression analysis to determine which properties were related to the critical value of Shields parameter. Based on the regression analysis, Wang (2013) proposed that the critical Shields parameter of a soil can be predicted by water content and clay size fraction of the soil as follows

$$\tau_{*c} = 8.46 - 27.76 \times w + 73.69 \times CSF + 83.22(w \times CSF) \tag{2.9}$$

where τ_{*c} is the Shields parameter, w is the water content (in decimal form), and CSF is the percentage of clay finer than 2 μm in the soil (in decimal form). Both Eqs. (2.7) and (2.9) can be converted to the critical shear stress from the definition of Shields' parameter:

$$\tau_c = \tau_{*c} \times (\gamma_s - \gamma) \times d_{50} \tag{2.10}$$

where τ_c is critical shear stress (Pa), τ_{*c} is the Shields parameter, γ_s is the specific weight of the soil (N/m^3), γ is the specific weight of water (N/m^3), and d_{50} is median particle diameter (m).

Development of Critical Shear Stress Erodibility Categories

As evaluated previously in this chapter, many researchers have attempted to predict the critical shear stress of soils through a wide variety of methods and based on numerous soil properties. More recently, a group of researchers have begun to divide the range of measured critical shear stress of soils into several large categories in order to identify soil type trends and distributions. Hanson and Simon (2001) were the first to divide their critical shear stress measurements into five groups. They used an in-situ jet to conduct field tests in order to determine the critical shear stresses of soils throughout the Midwest. The critical shear stresses were categorized into ranges of critical shear stresses and compared in order to identify trends among the various soil samples.

The work by Hanson and Simon (2001) was continued by Thoman and Niezgoda (2008) in the Powder River Basin in Wyoming where the in-situ jet test was also used to determine the critical shear stress of a variety of soil samples. The critical shear stresses were once again classified into five categories. However, the range of values of critical shear stress values for each category was different than the ranges used by Hanson and Simon (2001). Additionally, Thoman and Niezgoda (2008) took the division one step further by labeling each category of critical shear stress ranges from very erodible to very resistant, providing a new qualitative tool by which soil samples can be described. The divisions and category labels (very erodible to very resistant) created by Thoman and Niezgoda (2008) using the data from the Powder River Basin include the following: very erodible (0.01-0.374 Pa); erodible (0.375-1.99 Pa); moderately resistant (2.00-9.99 Pa); resistant (10.0-99.9 Pa); very resistant (>99.9 Pa).

Development of a Risk-Based Ranking System for Bridges

Another recent thrust of many researchers is to attempt to quantify the risk associated with a certain bridge in order to better prioritize operation and maintenance, thereby streamlining the use of funding. With over 400,000 bridges spanning water in just the United States and an unknown number of them vulnerable to scour (Stein et al., 1999), risk and reliability analyses are arising as a feasible method to identify the bridges that have the highest risk of failure in order to prioritize infrastructure investment and possibly justify the need for increased spending on maintenance (Khelifa et al., 2013). As noted by Niezgoda and Johnson (2007), risk requires two components in order to be determined: 1)

probability of failure (defined in terms of failure rates) and 2) consequences (defined in terms of failure rates). Currently, reliability studies are being used in hydraulic engineering to aid in decision making, determine the probability of failure of a structure, and determine the life expectancy of a hydraulic structure under uncertainty (Johnson, 1996). However, there is still a great deal of uncertainty surrounding these risk and reliability analyses. Additionally, there are several methods utilized in the literature including those based on the HYRISK model (Khelifa et al., 2013 and Stein et al., 1999), first order reliability method and sensitivity analysis (FORM) (Johnson, 1995 and 1996), risk priority numbers (RPN) (Johnson and Niezgoda, 2004; Niezgoda and Johnson, 2007 and 2012), benefit probability numbers (BPN) (Niezgoda and Johnson, 2012), and load and resistance factor design (LRFD) (Clopper and Lagasse 2011; Ghosn 2005). Each of these methods has its own uncertainties associated with it based on the parameters and scour formula utilized. However, this report will focus on the HYRISK model which provides the most seamless method for incorporating soil erodibility into the risk prediction.

The techniques developed by Khelifa et al. (2013) and Stein et al. (1999) are risk based models that utilize categories of the National Bridge Inventory (NBI) database to create a relative ranking of bridges according to risk of scour failure. Both studies are based on the Federal Highway Administration's (FHWA) model, HYRISK, which was developed in the late 1990's and updated in 2006.

The first steps are to calculate the rebuilding, running, and time loss cost. The following equations show those used by Stein et al. (1999)

$$Rebuilding\ Cost\ (\$) = C_1 WL \tag{2.11}$$

where C_1 is the unit rebuilding cost, W is the bridge width (NBI Item 52), and L is the bridge length (NBI Item 49).

$$Running\ Cost\ (\$) = C_2 DAd \tag{2.12}$$

where C_2 is the cost of running vehicle, D is the detour length (NBI Item 19), A is the average daily traffic (ADT) (NBI Item 29), and d is the duration of the detour in days (estimated from NBI Item 29).

$$Time\ Loss\ Cost\ (\$) = [C_3 O\left(1 - \frac{T}{100}\right) + C_4 \frac{T}{100}] \frac{DAd}{S} \tag{2.13}$$

where C_3 is the value of time per adult, O is the occupancy rate, T is the average daily truck traffic expressed as a percentage (NBI Item 109), C_4 is the value of time for a truck, and S is the average detour speed. The total cost is the sum of the three costs given in Eqs. (2.11) to (2.13). Next, the risk adjustment factor is calculated. The equation for the risk adjustment factor is

$$K = K_1 K_2 \tag{2.14}$$

where K is the risk adjustment factor, that is the product of K_1, a bridge-based factor and K_2, a soil-based factor. The recommended values for K_1 are

- 1.0 = simple spans
- 0.8 = continuous spans with lengths less than 30 m
- 0.67 = rigid continuous spans with lengths in excess of 30 m

The default value for K_2 is 1.0, but can be adjusted downward if foundation information is known. To date, K_2 has not been included in any application of HYRISK, as this adjustment factor needs to be based on soil properties that are not part of the NBI database, but rather found in state databases. Determining a set of adjustment factors of K_2 that relate to soil properties is one of the key objectives of this study.

The schematic shows that the next step is to determine the probability of failure, which is determined by combining the probability of failure given scour vulnerability and the overtopping frequency. The equation provided by Stein et al. (1999) for probability of failure is shown below, and the results of the calculations are noted in Table 2.9.

$$P\left(F\middle|(OT\ and\ SV)\right) = \sum_D P(D|OT)P[F|(SV\ and\ D)] \quad (2.15)$$

where F is failure, OT is the overtopping frequency, SV is the scour vulnerability, and D is the dimensionless depth (depth/overtopping depth). An example of one of the design tables used in Eq. (2.15) is shown in Table 2.9.

Table 2.9: Cost – Probability of failure given overtopping frequency and scour vulnerability (Stein and Sedmera, 2006). Source: Stein and Sedmera (2006), Table 12.

Scour vulnerability (Items 60 and 61)	Overtopping Frequency (Items 26 and 71)			
	Remote (0.01)	Slight (0.02)	Occasional (0.20)	Frequent (0.50)
0 (bridge failure)	1.00	1.00	1.00	1.00
1 (bridge closed)	0.01	0.01	0.01	0.01
2 (extremely vulnerable)	0.005	0.006	0.008	0.009
3 (unstable foundation)	0.0011	0.0013	0.0016	0.002
4 (action required)	0.0004	0.0005	0.0006	0.0007
5 (fair condition)	0.000007	0.000008	0.00004	0.00007
6 (satisfactory condition)	0.00018	0.00025	0.0004	0.0005
7 (good condition)	0.00018	0.00025	0.0004	0.0005
8 (very good condition)	0.000004	0.000005	0.00002	0.00004
9 (excellent condition)	0.0000025	0.000005	0.00002	0.00004

In earlier versions of the HYRISK model, the next step in the schematic requires the use of the bridge's age as a validation check on the probability of scour failure. It should be noted that not all versions of HYRISK have incorporated this age-adjustment factor. More recent versions, including that by Stein and Sedmera (2006) and Khelifia et al. (2013), have not applied adjustment factors for age. Based on Eq. (2.16) below, if the predicted age (X_{90}) is less than the actual age, then the probability of scour failure can be adjusted using Eq. (2.17).

$$X_{90} = \frac{\log(1-0.90)}{\log(1-P)} \tag{2.16}$$

$$X_{actual} = \frac{\log(1-0.90)}{\log(1-P_{update})} \tag{2.17}$$

where X_{90} is the 90th percentile mean time to scour failure, P is the initial probability of scour failure, X_{actual} is the actual age of the bridge according to the NBI database, and P_{update} is the downward adjusted probability if X_{90} is less than X_{actual}. Finally the schematic indicates that risk can be calculated by multiplying together the probability of failure (P), the risk adjustment factor (K), and the Cost.

Stein and Sedmera (2006) further refined many of the cost calculations, and proposed the following new Eqs. (2.18) – (2.21)

$$Rebuilding\ Cost\ (\$) = C_1 eWL \tag{2.18}$$

where C_1 is the rebuilding cost, W is the bridge width, L is the bridge length, and e is a cost multiplier for early replacement estimated from a (average daily traffic) and follows the relationship:

- e = 1.0 for $a < 100$
- e = 1.1 for $100 \leq a < 500$
- e = 1.25 for $500 \leq a < 1000$
- e = 1.5 for $1000 \leq a < 5000$
- e = 2.0 for $a \geq 5000$

$$Running\ Cost\ (\$) = \left[C_2\left(100 - \frac{T}{100}\right) + C_3\frac{T}{100}\right]DAd \tag{2.19}$$

where C_2 is the cost of running a vehicle, C_3 is the value of time per adult, T is the average daily truck traffic, D is the detour length, A is the average daily traffic, and d is the duration of the detour in days.

$$Time\ Loss\ Cost\ (\$) = \left[C_4 O\left(100 - \frac{T}{100}\right) + C_5 \frac{T}{100}\right] \frac{DAd}{S} \tag{2.20}$$

where C_4 is the value of time for a car, C_5 is the value of time for a truck, O is the average occupancy rate of a vehicle, and S is the average detour speed.

$$Life\ Lost\ Cost\ (\$) = C_6 X \tag{2.21}$$

where C_6 is the cost of lost life and X is the number of expected deaths.

Khelifa et al. (2013) made several additional modifications to the cost calculations in order to further refine the risk prediction. The new equations used by Khelifa et al. (2013) are

$$Rebuilding\ Cost\ (\$) = (C_0 + C_1) eWL \tag{2.22}$$

where C_o is the demolition cost, C_1 is the rebuilding cost, W is the bridge width, L is the bridge length, and e is a cost multiplier for early replacement estimated from a (average daily traffic) and follows the relationship provided for Eq. (2.18).

$$Life\ Lost\ Cost\ (\$) = C_6(TC)(AR)(O) \quad (2.23)$$

where C_6 is the cost of lost life, TC is the time to clear the bridge, and AR is the arrival rate of vehicles. Note that Eq. (2.23) differs from Eq. (2.21) in that it explicitly accounts for exposure, or the amount of time a vehicle spends traveling across a bridge. The other major update made by Khelifa et al. (2013) was to correct and update the probability of failure given overtopping frequency and scour vulnerability to ensure that all values were monotonically increasing as scour vulnerability and overtopping frequency were both increasing. The updated values are shown in Table 2.10.

Table 2.10: Probability of failure given overtopping frequency and scour vulnerability. Source: Khelifa et al. (2013), Table 2.

Scour vulnerability (Items 60 and 61)	Overtopping Frequency (Items 26 and 71)			
	Remote (0.01)	Slight (0.02)	Occasional (0.20)	Frequent (0.50)
0 (bridge failure)	1.00	1.00	1.00	1.00
1 (bridge closed)	0.01	0.01	0.01	0.01
2 (extremely vulnerable)	0.005	0.006	0.008	0.009
3 (unstable foundation)	0.0011	0.0013	0.0016	0.002
4 (action required)	0.0004	0.0005	0.0006	0.0007
5 (fair condition)	0.0003	0.0004	0.0005	0.0007
6 (satisfactory condition)	0.00018	0.00025	0.0004	0.0005
7 (good condition)	0.00018	0.00025	0.0004	0.0005
8 (very good condition)	0.000004	0.000005	0.00002	0.00004
9 (excellent condition)	0.0000025	0.000003	0.000004	0.000007

This framework is highly methodical, and after many years of development, it has been shown to produce reliable results. However, this method can only be used for relative ranking purposes for structures that are currently in existence. It cannot be used as a design tool or, in its current condition, to produce expected loss estimates that can be used in cost-benefit analysis to assess scour countermeasures.

Summary

In this chapter, five key concepts were introduced and explored. Initially, important soil properties and methods for classifying soils were examined which enabled a review of the second key point, a comparison of various methods used to measure the critical shear stress of soils. The third area explored was the specific method used by the Georgia Tech researchers to determine the critical shear stress of soil samples. The fourth section presented a conceptual framework for grouping ranges of soil critical shear stresses into a

broad set of erodibility categories that account for uncertainty in measurements and predictions, and finally, the fifth concept discussed the HYRISK model. All of these concepts set the stage for an in-depth analysis of the soil properties that affect critical shear stress which will enable researchers to create a set of K_2 risk adjustment factors for HYRISK, thereby allowing HYRISK to predict expected losses due to a scour failure as a function of (simple) soil properties available on boring logs.

CHAPTER 3

METHODOLOGY

This chapter describes the methodology developed to incorporate soil erodibiity characteristics into HYRISK. Figure 3.1 shows the process used to incorporate soil erodibility characteristics into HYRISK. The critical shear stress is an essential parameter in scour prediction formulas, and many researchers have developed equations to predict critical shear stress and resulting scour as a function of soil properties. Given the primary goal of these equations is to use them in bridge foundation design applications, the soil properties required as inputs to the equations tend to be very detailed.

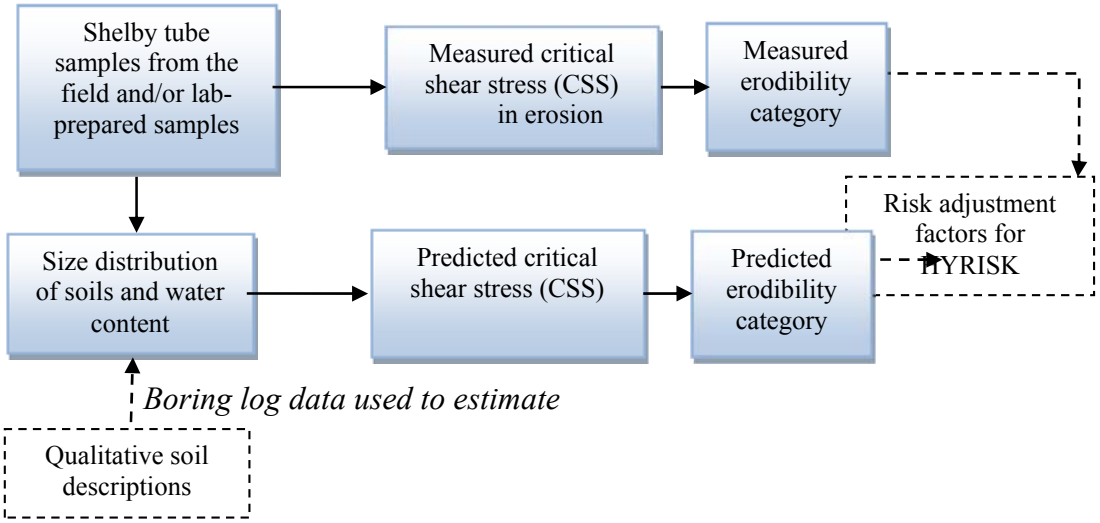

Figure 3.1: Process to link qualitative soil descriptions to HYRISK risk adjustment factors

For example, as described in Chapter 2, in prior research conducted at the Georgia Institute of Technology, Dr. Sturm and his graduate students developed regression

equations that predict critical shear stress and resulting scour as a function of two broad soil classifications: (1) coarse-grained soils such as sand, and (2) fine-grained soils such as silt and clay. In the first level of assessment shown in Figure 3.1, the researchers took Shelby tube samples from the field and tested the samples for erodibility as measured by the critical shear stress in a flume that had been designed specifically for that purpose. The researchers complemented these boring samples with experiments in which they prepared the soil samples to be tested; these experiments used lab mixtures of kaolin and ground silica of silt size to represent predominantly fine-grained soils representative of those found in Georgia in order to provide a wider range of soil properties than were obtained from the boring samples alone.

In the second level of assessment shown in Figure 3.1, the researchers used information about the size distribution of soils and water content measured from the Shelby tube and lab samples to develop equations to predict the critical shear stress. These relationships, shown in the shaded boxes in Figure 3.1, provide a method to relate soil characteristics such as water content and detailed size distributions, including clay content, percent fines (clay + silt), and median grain size to critical shear stress.

The capability to relate critical shear strength to soil erodibility properties is conceptually appealing, but unfortunately the soil properties used in these equations are available only for a small subset of bridges, i.e., this soil information is typically collected only during a Phase II scour evaluation. This prevents researchers from using these particular soil properties to develop a set of risk adjustment factors for HYRISK. However,

qualitative descriptions of soil properties based on visual and tactile assessments are available for each bridge in boring logs.

The question of interest for this project, shown in the third level of assessment in Figure 3.1 with a dotted line connecting it to the first and second level assessments, is to determine how to relate qualitative soil descriptions from boring logs to known soil erodibility properties. By categorizing soils into a small number of erodibility categories, the researchers were able to develop a set of risk adjustment factors for HYRISK. In turn, this allowed the researchers to rank bridges that should be targeted for a Phase I scour evaluation. The ranking developed in this paper is based on estimating the probability of failure (including the influence of soil erodibility properties) and expected economic losses.

Data used to relate critical shear stress to properties of soils

The data used in this study comes from two theses and one dissertation completed under the direction of Dr. Terry Sturm: Navarro (2004), Hobson (2008), and Wang (2013). Navarro collected field soil samples in partnership with the Georgia Department of Transportation (GDOT) in 2004. Hobson later collected additional field soil samples in partnership with GDOT in 2008, choosing samples that would complement Navarro's samples. Based on the limited number of fine-grained soil samples collected by Navarro and Hobson, Wang (2013) built upon their research by focusing only on fine-grained soils. Rather than collecting field samples, Wang (2013) mixed silt and clay size particles in the lab. The specimens were prepared by mixing Georgia kaolin and ground silica in varying

proportions by dry weight to create different samples for testing. Water was added into the sediment mixture at a ratio of 160 ml of water to 100 g of sediments. After thoroughly mixing the sediment and water sample, the suspension was transferred to a Shelby tube where it was allowed to settle for approximately 24 hours prior to erosion testing. Sediment mixtures of 10%, 20%, 40%, 60%, and 100% kaolin by dry weight were tested by Wang using the same open channel erosion flume as Navarro and Hobson to determine the critical shear stress.

In total, Navarro and Hobson (denoted as N/H on figures and tables) tested 46 samples and Wang (denoted as W on figures and tables) tested 22 samples. Based on a dimensional analysis of the initiation of motion problem in sediment transport, critical shear stresses were converted to the critical value of the dimensionless Shields parameter which is a measure of the ratio of shear force initiating sediment motion to the reference gravity force resisting motion given by (Sturm 2010):

$$\tau_{*c} = \frac{\tau_c}{(\gamma_s - \gamma) d_{50}} = \frac{\tau_c}{(SG - 1) \gamma d_{50}} \tag{3.1}$$

in which τ_c is the critical shear stress, γ_s is the specific weight of the soil grains, γ is the specific weight of water, SG is the specific gravity of the soil grains and d_{50} is the median grain size.

From their field data, Navarro and Hobson employed stepwise regression analysis to obtain the following relationship between the soil properties of 46 Shelby tube samples and the critical Shields parameter:

$$\tau_{*c} = 0.644 \times 10^{2.68 \times Fines} \times d_*^{-0.409} \tag{3.2}$$

where τ_{*c} is the critical value of the Shields parameter, *Fines* is the percent of fines (silt + clay) in a soil sample (in decimal form), and d_* is the nondimensional grain size defined by

$$d_* = \left[\frac{(SG-1)gd_{50}^3}{\nu^2} \right]^{1/3} \tag{3.3}$$

in which v is the kinematic viscosity of the water. The field soil samples on which Eq. (3.2) is based were predominantly in the silt and sand size ranges with 0.04 mm $\leq d_{50} \leq$ 2 mm and $0.05 \leq Fines \leq 0.7$.

Wang (2013) applied stepwise regression analysis to the flume test results for 22 experimental, artificially-mixed soil samples of kaolin and crushed quartz and obtained the following relationship for the Shields parameter:

$$\tau_{*_c} = 8.46 - 27.76 \times w + 73.69 \times CSF + 83.22(w \times CSF) \tag{3.4}$$

where w is the water content (in decimal form), and *CSF* is the percentage of clay size fraction by weight in the soil finer than d_{50} = 0.002 mm (in decimal form). Eq. (3.4) is appropriate to use for fine-grained soils with $d_{50} <$ 0.04 mm.

Consistent with other researchers (e.g., see Hanson and Simon 2001; Thoman and Niezgoda 2008), Sturm et al. 2008 divided the range of measured critical shear stress of soils into several categories and labeled each category from very erodible to very resistant, providing a qualitative tool by which erodibility of soil samples can be described. The erodibility categories and their critical shear stress ranges were modified slightly for this study based on the available Georgia data and are shown in Table 3.1.

Table 3.1: Shear stress ranges for each erodibility category and corresponding HYRISK K_2 factor

Erodibility Category	Critical Shear Stress Range (Pa)	K_2
Very Erodible	[0.1-0.5)	1.0
Erodible	[0.5-3.5)	0.8
Moderately Resistant	[3.5-8.0)	0.6
Resistant	[8.0-21)	0.4
Very Resistant	≥21.0	0.2

Note: K_2=1 for soils with unknown foundations

The association of ranges of critical shear stress with erodibility categories provides a convenient way to incorporate soil erodibility information into HYRISK. When HYRISK was originally designed it included a downward risk adjustment factor, K_2, based on a foundation-type factor (Stein, et al. 1999). Stein proposed five values for K_2, ranging from a value of 1.0 for unknown foundations or erodible soils to 0.2 for foundations on massive rock. A similar logic can be used to assign K_2 factors based on erodibility categories, as shown in Table 3.1. That is, Table 3.1 associates the critical shear stress ranges and erodibility categories with five K_2 HYRISK risk adjustment factors. The question of interest, then, becomes how to associate soil classifications found on boring logs to these erodibility factors in order to apply a K_2 factor in HYRISK.

Methodology

Different soil classification systems have been developed to describe the division between fine and coarse grained soils. Given that GDOT uses the Unified Soil Classification System (USCS) for their boring logs, this methodology applies the USCS as refined in ASTM D 2487-11 (ASTM International 2011a). In this system, coarse-grained

soils are defined as those having more than 50% by weight retained on the No. 200 sieve (0.075 mm), while fine-grained soils (silt and clay) are those with more than 50% by weight passing the No. 200 sieve. Sand is defined as soil grains retained on the No. 200 sieve but passing the No. 4 sieve (4.75 mm), while gravel is retained on the No. 4 sieve but passes the 75-mm sieve. The methodology for associating erodibility categories with soils differs for coarse-grained soils that are clean sand or gravel, coarse-grained soils that are a mix of sand or gravel with fines consisting of silt and clay, and fine-grained soils composed predominantly of silt and clay.

Associating erodibility categories with coarse-grained soils that are clean sand or gravel

For coarse-grained soils that are clean sand or gravel, Shields' diagram (Sturm 2010) should be used to find the critical shear stress. Shields' diagram provides an accepted, well-established experimental relationship between τ_{*c} and d_* based on the results of many investigators. The value of d_* as defined by Eq. (3.3) depends primarily on d_{50} and known properties of water and specific gravity of sand and gravel. Shields' diagram provides the corresponding value of τ_{*c} = f (d_*) from which the critical shear stress τ_c follows directly from the definition given by Eq. (3.1). For the USCS, coarse–grained classifications of SW or SP (well-graded or poorly graded sand) and GW or GP (well-graded or poorly-graded gravel), critical shear stress is calculated from Shields' diagram, because *Fines* are less than 5%. The value of τ_c determines the erodibility category as shown in Table 3.2. The sand classification is based on a minimum size of 0.075 mm while for gravel, a minimum size of 4.75 mm is used according to the USCS. The resulting

erodibility classifications are conservative in that larger sizes have higher critical shear stresses and are less erodible. As an example, the value of d_* from Eq. (3.3) for groups SW or SP in Table 3.2 is 1.9 with d_{50} = 0.075 mm, SG = 2.65 for quartz and $\nu = 1\times10^{-6}$ m^2/s for water. Shields' diagram gives the value of τ_{*c} = 0.1 from which τ_c = 0.12 Pa (very erodible) according to Eq. (3.1) with γ = 9810 N/m^3 for water.

Table 3.2: Categories of critical shear stress determined from Shields' diagram or Eq. (3.2).

USCS Soil Type	d_{50} (mm)	d_*	Fines %	Critical Shear Stress (Pa)	Erodibility Class Used in HYRISK
SW & SP	0.075	1.9	0	0.12	Very Erodible
SW-SM, SW-SC, SP-SM, & SP-SC	0.075	1.9	5	0.82	Erodible
SM, SC, & SC-SM	0.075	1.9	12	1.3	Erodible
GW & GP	4.75	120	0	3.5	Moderately Resistant
GW-GM, GW-GC, GP-GM, & GP-GC	4.75	120	5	9.5	Resistant
GM, GC, & GC-GM	4.75	120	12	14.7	Resistant

Associating erodibility categories with coarse-grained soils that are a mix of sand or gravel with fines

The authors' methodology assigns an erodibility category for coarse-grained soils that are a mix of sand or gravel with *Fines* in the ranges of 5%-12%, or >12% using the Navarro/Hobson relationship (Eq. (3.2)) instead of Shields' diagram. Eq. (3.2) determines the critical Shields parameter and critical shear stress as a function of the fraction by weight of *Fines* and median grain size, d_{50}. In Table 3.3, the letters C and M follow the designation

of sand (S) or gravel (G) to indicate whether *Fines* are predominantly clay or silt, respectively. To obtain τ_c, Eq. (3.2) is applied with the minimum size cutoff for sand or gravel depending on which comprises a higher percentage of the sample by weight. Similarly, *Fines* are taken as 5% for the 5%-12% group and 12% for the >12% group in Eq. (3.2) to obtain the most conservative estimate of erodibility category in Table 3.3.

As an example of the application of Eq. (3.2) when *Fines* are present, consider the group SM or SC in Table 3.3 with *Fines* >12%. Using the minimum size for sand of d_{50} = 0.075 mm, d_* = 0.19 as for the groups of SW or SP given previously. Then this value of d_* and *Fines* = 0.12 are substituted into Eq. (3.2) for SM or SC to obtain τ_{*c} = 1.0 from which the definition in Eq. (3.1) yields τ_c = 1.3 Pa (erodible) as shown in Table 3.3.

Table 3.3.: Mapping of erodibility categories onto plasticity chart for fine-grained soils

USCS Soil Group	Name (ASTM 2487)	Description (Sowers 1979)	Erodibility Category
CL	Lean clay	Low plasticity clays, sandy or silty clays	Erodible
CL-ML	Silty clay	Silty clays	Erodible
ML	Silt	Silts, very fine sands, silty or clayey fine sands, micaceous silts	Moderately Resistant
MH	Elastic silt	Micaceous silts, diatomaceous silts	Resistant
CH	Fat clay	Highly plastic clays, sandy clays	Resistant

The procedure just outlined for clean sand or gravel, and sand or gravel with fines, can be repeated for each sand and gravel group to assign an erodibility category. For

HYRISK and other scour risk assessment tools, the most conservative erodibility category should be assigned to each soil group, i.e., the soil group that corresponds to the minimum calculated critical shear stress. Even if the soil group extends across more than one erodibility category, it is assigned the more erodible category as a conservative estimate. For example, if d_{50} of the group SM with >12% Fines is 1.0 mm, the erodibility category in Table 3.3 would change from erodible to moderately resistant, but the category of erodible would be the one retained assuming that the particle size distribution and thus the value of d_{50} is not available from the field boring logs. In this case, HYRISK would assign a K_2 value of 0.8, corresponding to the erodible category. Consequently, bridges with this assignment of K_2 would receive a lower priority ranking for a Phase I screening or Phase II evaluation. In other cases such as the SW and SP soils, four erodibility categories (very erodible, erodible, moderately resistant, and resistant) can occur over the full range of sand sizes. For these two soil groups, the USCS group designation alone from a field evaluation provides insufficient information about soil erodibility (i.e., a size distribution, which is unlikely to be found on boring logs, is needed to narrow the erodibility group albeit a description of the soil as fine (0.075-0.425 mm), medium (0.425 mm-2.0 mm) or coarse (2.0 mm-4.75 mm) sand could be helpful). In this instance, HYRISK would assign a K_2 value of 1.0, corresponding to a very erodible category. Consequently, the expected loss associated with scour failure would not change, since it is uncertain just from the USCS group designation alone how susceptible these bridges are to scour.

Associating erodibility categories with fine-grained soils

Characterization of the engineering properties of fine-grained soils is often achieved by laboratory measurement of the Atterberg limits of liquid limit (w_{LL}) and plastic limit (w_{PL}), which define for decreasing water content the water content at which the soil transitions from a viscous liquid to a plastic solid, and the water content limit between a plastic solid and a semisolid subject to brittle fracture, respectively. The difference between these two index properties is defined as the plasticity index (I_P) which measures the range of water content over which the soil exhibits plastic properties. The soil index properties of I_P vs. w_{LL} are plotted in the plasticity chart shown in Figure 3.2 which becomes the basis for defining soil groups for fine-grained soils in the USCS. Clay (C) is defined as plotting above the "A line" while silt (M) and organic soil (O) plot below it. Highly plastic behavior for clays or high compressibility for silts is indicated by H for $w_{LL} \geq 50\%$ while a lower level of plasticity or compressibility is signified by L for $w_{LL} < 50\%$.

One difficulty posed by this approach for the authors' particular research objective of estimating erodibility from field observations alone is that the liquid limit and plasticity index may not be provided in boring logs, although one of the fine-grained soil groups identified in Figure 3.2 may be estimated using visual and manual classification techniques from ASTM D2488a (ASTM International 2011b) and reported in the field log. Additionally, previous literature has indicated that liquid limit and plasticity index may be unreliable quantitative indicators of soil erodibility thresholds or erosion rates. (Partheniades 2010, Grabowski et al. 2011).

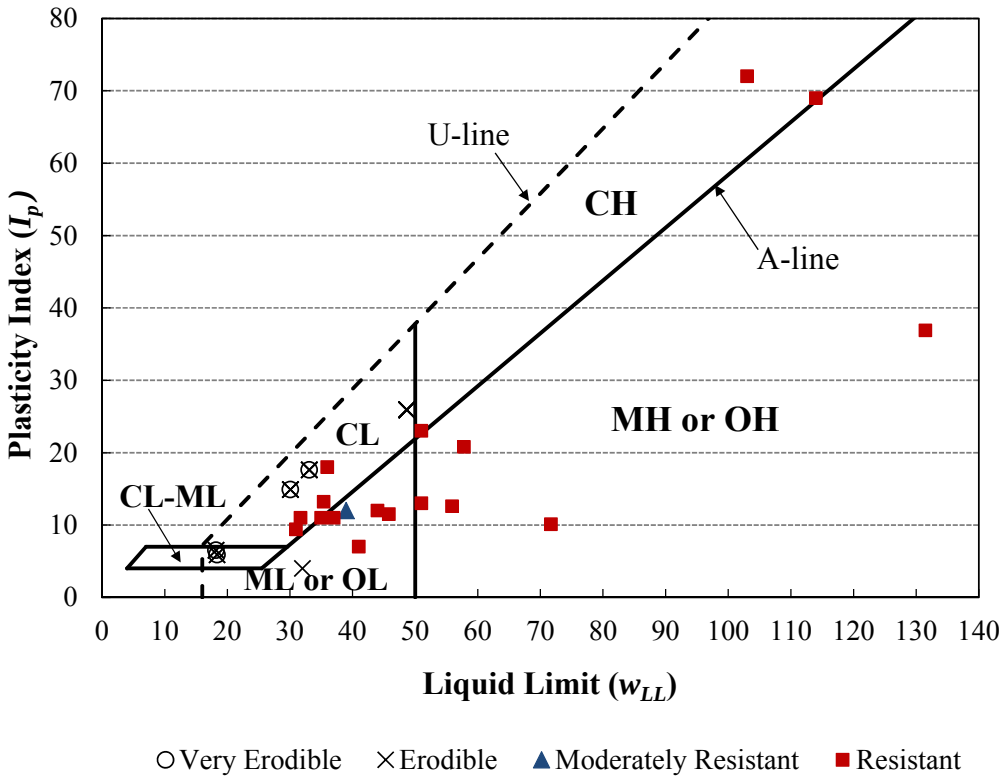

Figure 3.2. Mapping of soil erodibility categories onto plasticity chart.

In spite of these caveats, the utility of the plasticity chart was explored in this study for a broad classification of field data into erodibility categories when the only information available is a field estimate of USCS soil group. For this purpose, measured I_P and w_{LL} for the fine-grained field soils and the lab mixtures of soils, all of which were fine-grained, are plotted in Figure 3.2 with the erodibility category based on measured τ_c indicated by symbol shape. Erodibility categories that correspond with the soil groups from the plasticity chart are shown in Table 3.3. For CH and MH groups, all field data points, although they are limited in number, can be categorized as very resistant. In the silty clay group (CL-ML), all data points are either very erodible or erodible. However, the very erodible data resulted from erosion of a thin fluff layer from the kaolin lab mixtures at the

surface of the soil core, and so are not really representative of field scour conditions. For this reason the CL-ML group is taken as erodible in Table 3.3. The ML group incorporates predominantly resistant data points with the addition of one erodible and one moderately resistant data point. The erodible data point is a sandy silt with very low plasticity index and is a borderline coarse-grained soil with 49% sand and essentially no clay. The moderately resistant data point has a critical shear stress of about 5 Pa while the resistant data have critical shear stresses in the range of 11 to 17 Pa which are in the lower range of the resistant category. To be on the conservative side as in the coarse-grained soil classifications of erodibility category, the ML group is designated as moderately resistant.

The most difficult correspondence between erosion category and soil group is presented by the CL group. Discounting the very erodible data points again as unrepresentative of the field, the erodibility category is either erodible or resistant, and neither is dominant. The value of I_P for these data points is similar which implies that they have similar values of clay-size fraction (*CSF*) as expected from previous positive correlations of increasing *CSF* with increasing I_P (Jacobs et al. 2011, Wang 2013). As shown by Eq. (3.4), *CSF* is a significant predictor variable for τ_c. The other important predictor variable in Eq. (3.4) is water content which is not given in a plasticity chart, but it is this variable that probably accounts for the difference in erodibility categories for the CL group. Water contents are greater than about 100% for the erodible data points and less than approximately 30% for the resistant points in the CL group. Increasing water content is predicted by Eq. (3.4) to reduce τ_c for a given *CSF* which is consistent with the erodible data points in the CL group all of which have a high water content. Thus, in the

absence of field data on water content, the CL group is taken as erodible to minimize risk as shown in Table 3.3.

Organic content can significantly alter the erodibility of a soil because it can affect the interparticle bonds that make a fine-grained soil cohesive. No organic matter was added to the laboratory-mixed soil samples, and the field data all showed either zero or very low organic contents. Accordingly, no attempt is made to place OH and OL soil groups into erodibility categories in Table 3.3.

Summary of methodology

To apply the researchers' methodology to HYRISK, the soil sample must be divided into either fine or coarse grained soils as indicated by the USCS soil group identification in the field notes and boring log. Then, Tables 3.2 and 3.3 are used to assign an erodibility category based on the USCS group classification, and Table 3.1 provides a corresponding K_2 adjustment factor to be employed in HYRISK. In some cases, the field data included a size distribution and water content so that Eqs. (3.2) and (3.4) could be used for a more accurate assignment of erodibility category.

CHAPTER 4

APPLICATION TO HYRISK

The depth of a scour hole around a foundation is determined by the complex interaction of the water moving over the soil surrounding the foundation. Although this interaction is not fully understood, the two main components that affect the scour depth are the motion of the water and the properties of the soil. A better understanding of a soil's resistance to erosion allows engineers to: 1) create improved bridge designs; and 2) identify those bridges that are most likely to be affected by scour action. This section will focus on the second point by integrating the predicted critical shear stress of a soil with the HYRISK model discussed in the Literature Review. By incorporating soil erodibility categories into HYRISK, more accurate prioritizations for bridge maintenance can be achieved, and resources and be more efficiently distributed to ensure bridge safety. When HYRISK was originally designed it included a downward risk adjustment factor, K_2, that is based on a foundation-type factor (Stein et al.,1999). Stein et al. (1999) suggests that the following downward adjustment factors:

- 1.0 = Unknown foundation or spread footing on erodible soil above scour depth; pier footing top visible or 0.3-0.6 m below streambed
- 0.8 = Pile foundation of unknown length or when length is known to be <6 m in depth or all wood pile foundations
- 0.5 = Pile foundations with lengths in excess of 6 m below present stream bottom
- 0.2 = Foundations on massive rock.

However, Stein et al. (1999) notes that this information is not available on a national level and must be procured on a state-by-state basis. Due to the importance of soil erodibility on the scour depth, this study elected to use GDOT soils data collected from state boring logs to create the downward adjustment factor, K_2, for HYRISK using the state of Georgia as an example case. For the purposes of this report, the following adjustment factors are recommended for K_2:

- 1.0 = Unknown or very erodible soil
- 0.8 = Erodible soil
- 0.6 = Moderately resistant soil
- 0.4 = Resistant soil
- 0.2 = Foundations on massive rock.

The next sections explain how the HYRISK model was adjusted for Georgia and describe challenges faced during the data collection and analysis phases. The final results for the re-ranking of the most at-risk bridges in Georgia are presented and discussed.

Data Collection of Soil Boring Logs

The data used in the HYRISK analysis were collected from boring logs provided by GDOT. In total, 41 boring logs were used in this report. A "top 100" list of at-risk bridges in Georgia was identified using a HYRISK assessment that excluded soil erodibility factors. The most at-risk bridges were identified by ranking bridges according to two separate criteria: 1) those with the highest probability of failure; and, 2) those with the expected cost of failure. There were a large number of bridges that were ranked in the

"top 100" lists associated with each criterion. When the lists for both at-risk categories were combined, there were potentially 133 bridges that could be used in the analysis. All of the bridges used in the analysis were identified using HYRISK and were not from any of the lab samples.

However, differences between the national and state organizational schema limited the number of boring logs for bridges that could be located. Of the original 133 bridges, approximately 50 could be located, and of those bridges, 41 had boring logs in their file. Therefore, 41 bridges were used as a sample in the HYRISK comparison. For each bridge there were anywhere from two to more than 20 boring logs, and the borings ranged in depth from five feet to over a hundred feet. Additionally, each boring log provided varying amounts of information. At a minimum, a soil description was provided, and in 80% of the logs, a USCS soil type was also provided. A grain size distribution was available on 37% of boring logs, water content was available for 22%, and clay percent was available for just 12%. The number of soil samples tested from borings also varied.

Data Analysis of Soil Boring Logs

Once the boring logs were acquired, the data needed to determine the erodibility category of each boring was compiled. However, using boring logs to determine the dominant erodibility category of the soil at a bridge foundation is not necessarily a straightforward process.

Figure 4.1 of a sample boring log demonstrates the steps used to determine the erodibility of a particular boring. The information at the top of Figure 4.1 is information

about where, when, how, and by whom the boring was done. All the information about the boring is contained in the columns below the header. The column to the far left is labeled "Elevation" in this boring log, but it can also be labeled "Depth". Both provide information about the thickness of soil layers in a boring. The next column to the right is labeled "Strata Description" and simply provides a visual description by the operator of the soil. The next column, which is unlabeled in this sample log, provides the visual representation of the USCS soil type that is associated with the column to its right. The USCS soil type is determined by the operator based on visual and textural indicators as the soil is extracted from the boring. The next column is labeled "Sample No." and shows where specific samples of soil have been extracted to use for further laboratory tests. These further tests usually provide information about grain distributions, clay percentages, water contents, and other soil properties. Not all boring logs collect samples for further lab testing. For these cases, the "Sample No." column would be empty. The next column is labeled "SPT" which stands for standard penetration test. This test is performed by driving a hollow tube through the soil, and the number provided in the SPT column is the number of blows required to advance the tube six inches into the soil. The SPT test is used as a measurement of soil density, and although this test is provided for almost every boring, it has little connection to the critical shear stress of a soil. The remaining columns are for tests that rarely occur in the field but include: 1) Unit Wt.; 2) % Moist.; 3) LL (w_{LL}) ; 4) PI (w_{PL}); 5) % Pass 75μ; 6) Rock RQD; and, 7) % Rock Rec. These abbreviations stand for: 1) unit weight of soil; 2) water content; 3) liquid limit; 4) plasticity index; 5) percent of fines in soil; 6) rock quality designation; and, 7) the percentage of rock recovered from the boring. All of these

measures have been discussed previously except for those involving rock samples. The percentage of rock recovered from the boring hole is the amount of rock extracted from the boring hole compared to the total volume of the rock that was drilled to advance the bore hole. The rock quality designation is a measure of the jointing or fracturing in a rock mass with high quality rock having less fracturing.

The sample boring log shown in the figure helps explain why it is not always a straightforward process to determine the erodibility of the soil around a bridge. The soil types encountered in this sample boring log include, sand, silt, and clay which each possess very different properties that affect critical shear stress. Additionally, the top one or two layers cannot simply be examined to determine the critical shear stress because if a scour hole develops around the pier it could expose soil layers at further depths which could be more or less resistant to scour. Therefore, a boring log must be looked at holistically, and the soil with the lowest critical shear stress, and most likely to be eroded, sets the limit for erodibility category of the boring. For instance, if a boring contained three different soil types that were resistant, moderately resistant, and very erodible, then the entire boring would be labeled as very erodible. This is a conservative method of ensuring that a new bridge is not under designed or that the risk of scour to an existing bridge is under predicted.

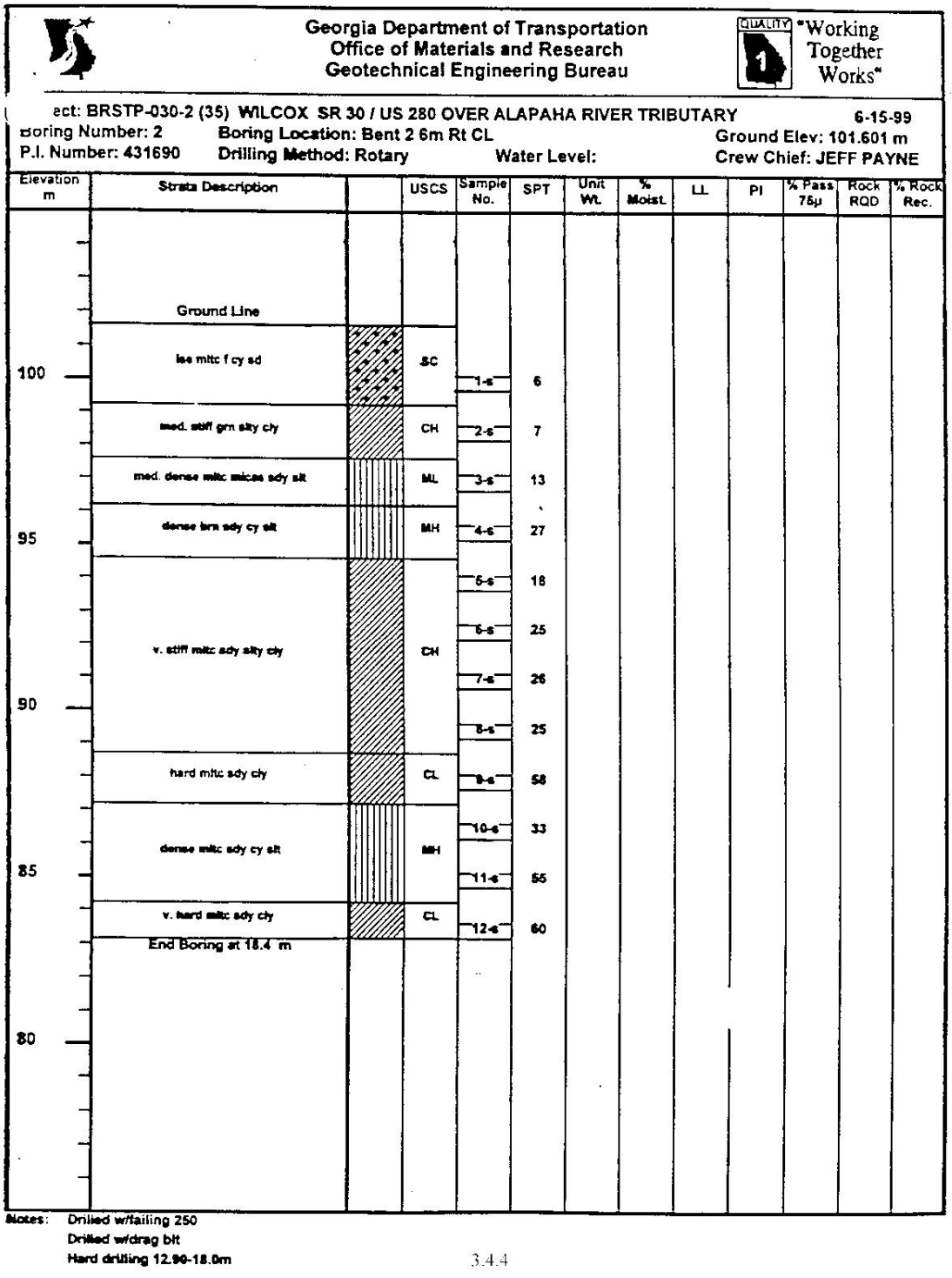

Figure 4.1: Sample boring log.

The methodology from Chapter 3 is applied to the GDOT boring logs in order to predict the dominant erodibility category of each bridge. Table 4.1 provides an example of the digitized boring logs from a bridge in Georgia.

Table 4.1: Digitized boring log for Glisson Road Bridge over Wolfe River in Candler County, GA.

Station: 19+92 Cl			Station: 20+52 Cl			Station: 21+72 Cl		
Depth (ft)	USCS	Wat Cont*	Depth (ft)	USCS	Wat Cont*	Depth (ft)	USCS	Wat Cont*
11	SC	--	9	CL	--	6	SC	--
26	CL	20	22.5	SC	36	12	SP	--
41	SP	--	26	SP	--	27	SM	31
50	MH	48	55	SM	28	37	SC	30
						50	MH	22

*Note: "Wat Cont" indicates water content.

Similarly to the sample boring log, there are a wide range of soil types that are found in the area surrounding the bridge. Note that the USCS soil type SP (poorly-graded sand) has an erodibility category of "very erodible." Based purely on the boring log data, the K_2 value assigned to this bridge would be 1.0 which represents very erodible.

Another limitation to make note of in Table 4.2 is that some median grain diameters are listed as simply "<0.075mm". This indicates that greater than fifty percent of the soil particles were smaller than the No. 200 sieve (which has a diameter of 0.075 mm). Since no smaller divisions in grain size were made beyond the No. 200 sieve, there is no way to determine the median grain size. Therefore, the median grain size has been stated as <0.075 mm and cannot be used in either the Wang or Navarro/Hobson equation which both require knowledge of the median grain size to convert the Shields parameter to the critical shear

stress value. However, there is additional lab data for this bridge which is shown in Table 4.2.

Table 4.2: Lab data and critical shear stress calculations for Flisson Road over Wolfe River in Candler County, GA.

Station	Dpth (ft)	US CS	d_{50} (mm)	% Fine	Water Content	w_{LL} %	I_p %	Clay %	d_*	CSS* Wang	Erod Wang	CSS* N/H	Erod N/H
DO-3	13.5	CL	<0.075	54.2	23.1	48	21	42	--	--	--	--	--
DO-5	23.5	SC	0.13	36.1	13.9	39	14	23	3.28	51.0	Res	7.74	Mod Res
DO-9	43.5-45	MH	<0.075	78.3	47.0	86	31	49	--	--	--	--	--
DO-4	18.5	SC	0.09	43.5	34.3	45	19	23.5	2.27	33.5	Res	9.83	Res
DO-6	28.5	SM	0.14	22.9	24.4	29	6	11.5	3.53	28.3	Res	3.58	Mod Res
DO-8	38.5	SM	0.11	43.8	29.2	49	15	35	2.78	61.7	Res	11.3	Res
DO-4	18.5	SM	0.08	47.4	31.9	49	20	25	2.02	31.9	Res	11.7	Res
DO-6	28.5	SC	0.087	45.6	31.8	46	20	34.5	2.19	48.2	Res	11.0	Res
DO-9	43.5	MH	<0.075	72.0	22.7	55	19	42	--	--	--	--	--

*Note: CSS stands for the predicted critical shear stress of the soil sample using the specified equation.

When possible, lab data should be used to select the erodibility category instead of using boring log data which tends to be conservative due to the variation of erodibility categories seen even within one soil type. Since a majority of the median grain sizes for this bridge are greater than 0.04 mm, then the Navarro/Hobson equation should be used, which predicts that the erodibility category will be moderately resistant. For the Glisson Road Bridge over the Wolfe River, an erodibility category of moderately resistant, with an associated K_2 value of 0.6, is recommended for assessment purposes.

HYRISK Application

As described in Chapter 2, HYRISK is a risk-based model that is similar in concept to models used in other engineering applications, most notably earthquake engineering

(e.g., see Adachi and Ellingwood (2010); Ellingwood (2000); Ivey, et al. (2010)). HYRISK predicts the expected annual loss due to scour for each bridge as:

$$\text{Expected Annual Loss} = KP \times Cost \tag{4.1}$$

where K is the risk adjustment factor, P is the probability of bridge failure and $Cost$ is expected economic losses. The HYRISK methodology permits a downward adjustment of failure probabilities based on bridge-type factors or foundation-type factors. The risk adjustment factor, K, is given as:

$$K = K_1 K_2 \tag{4.2}$$

where K_1 = bridge-type factor (default is 1.0 for highest risk, i.e., no downward risk adjustment) and K_2 = foundation-type factor from state databases (default is also 1.0 with no downward risk adjustment).

This study uses a version of HYRISK that has been customized for Georgia (see Khelifa, et al. (2013) for details). This section examines how the expected annual losses (and associated ranking of bridges) changes when a K_2 risk adjustment factor is included.

Results

Table 4.3 summarizes the results of three HYRISK analyses. The first "original" analysis ranks bridges without incorporating soil erodibility properties. The second "USCS" analysis is based on the researchers' method that uses only information about the USCS soil group categorization to assign K_2 risk adjustment factors. The third "N/H and Wang" analysis uses Eqs. (3.2) and (3.4) to assign K_2 factors for the subset of bridges for which detailed soil property information was available including size distribution and water

content. Although the approach using the Navarro/Hobson and Wang equations is not the focus of this paper (as it requires detailed soil property information, which limits its applicability using only information available on boring logs), it provides a useful way to assess the second method based solely on USCS soil group classifications.

Table 4.3: Comparison of rankings - GA bridges with and without soil erodibility factors

Original Rank	Updated Rank USCS	Updated Rank N/H & Wang	K_2 USCS	K_2 N/H or Wang	Original Expected Loss	Expected Loss USCS ($)	Expected Loss - N/H and Wang ($)
1	1	1	1	1	438,169	438,169	438,169
2	2	11	1	0.4	203,314	203,314	81,326
3	3	2	1	1	162,464	162,464	162,464
4	4	26	1	0.4	153,986	153,986	61,594
5	5	3	1	1	129,378	129,378	129,378
6	6	6	1	0.8	118,332	118,332	94,665
7	7	4	1	1	116,918	116,918	116,918
8	8	5	1	1	112,914	112,914	112,914
9	9	24	1	0.6	104,973	104,973	62,984
10	10	25	1	0.6	103,322	103,322	61,993
11	22	29	0.8	0.6	93,516	74,812	56,109
12	11	7	1	1	90,601	90,601	90,601
13	12	8	1	1	87,670	87,670	87,670
14	29	9	0.8	1	86,512	69,210	86,512
15	13	10	1	1	86,196	86,196	86,196
16	14	31	1	0.6	84,500	84,500	50,700
17	15	23	1	0.8	79,744	79,744	63,795
18	16	12	1	1	79,319	79,319	79,319
19	17	13	1	1	78,638	78,638	78,638
20	18	14	1	1	78,207	78,207	78,207
21	19	15	1	1	77,177	77,177	77,177
22	20	16	1	1	76,522	76,522	76,522
23	21	17	1	1	76,049	76,049	76,049
24	30	27	0.8	0.8	75,789	60,631	60,631
25	23	18	1	1	74,567	74,567	74,567
26	24	28	1	0.8	72,941	72,941	58,353
27	25	19	1	1	71,793	71,793	71,793
28	26	20	1	1	71,317	71,317	71,317
29	27	21	1	1	70,318	70,318	70,318
30	28	22	1	1	70,214	70,214	70,214
31	32	36	0.8	0.4	64,862	51,889	25,945
32	34	33	0.8	0.8	56,366	45,093	45,093
33	31	30	1	1	52,630	52,630	52,630
34	33	32	1	1	47,955	47,955	47,955
35	35	34	1	0.8	38,670	38,670	30,936
36	36	35	1	0.8	35,444	35,444	28,355
37	37	37	1	0.8	18,724	18,724	14,979
38	38	38	1	1	10,183	10,183	10,183

The Navarro/Hobson and Wang equations could be applied to 15 (39%) of the 38 bridges. Values of K_2 in the "N/H or Wang" column that have been assigned a default value of 1.0 signify that the necessary data to use this method were unavailable. For cases in which data were available to compute the Navarro/Hobson or Wang equations, the K_2 risk adjustment factor computed from the Navarro/Hobson and Wang equations is always equal to or less than then K_2 risk adjustment factor computed using the USCS soil classification. Intuitively, this is because incorporation of more detailed soil property information in the Navarro/Hobson and Wang equations provides a more accurate prediction of the soil erodibility category which allows the engineer to have more confidence that the soil can be assigned a smaller K_2 risk-adjustment factor than the more conservative USCS method would allow in some cases. The inclusion of risk adjustment factors that account for soil erodibility categories impacts the ranking of bridges. The updated ranking is now a function of soil erodibility categories which affect the probability of failure and ultimately the expected loss in the event of bridge failure. For some bridges, such as the one that was originally ranked second, the original expected loss is so large ($203K) that the K_2 factor of 0.4 only changes the ranking from 2nd to 11th. Conversely, for the bridge that was originally ranked 4th, the K_2 factor of 0.4 has a larger impact on the rank which moves from 4th vs. 26th. The method based on Navarro/Hobson and Wang has a more influential impact on bridge rankings, with five out of the 15 bridges (or 33%) experiencing a change in rank of 36-50%. This is expected, given the method based on Navarro/Hobson incorporates more detailed soil property information.

CHAPTER 5

CONCLUSION

Scouring around foundations is the most common cause of bridge failures (Arneson et al., 2012). In the past twenty years, Georgia has experienced two major flooding events that have damaged hundreds of bridges and caused the deaths of 36 people (Gotvald et al., 2010; CDC, 1994; Cook et al., 2009). In addition to the loss-of-life cost of bridge failures, total damages from scour in the past twenty years in Georgia have been in excess of $300 million (Arneson et al., 2012; Gotvald et al., 2010). Due to the intensity of recent floods in Georgia (as well as other states) and the high cost in lives and resources, identifying those bridges that are most at risk to fail due to scour and ensuring future bridge design guidelines properly account for increased intensity and frequency of rainfall events are major areas of research.

For years, many researchers have called for new design standards that are strong enough to ensure bridge reliability during more intense and frequent weather events (IPCC, 2007; U.S. DOT, 2006 as referenced in Schmidt, 2008). To develop stronger design standards, it is paramount to better understand both the hydrodynamics which cause scour and the physical properties of soils that resist scour. This report developed an improved understanding of how scour occurs – and under what conditions – allowing researchers to develop more robust bridge design standards for *future* construction. Additionally, the report proposed a relationship between scour and soil properties that are routinely recorded on boring logs to better assess scour failure risks associated with *existing* bridge infrastructure.

Since scour around a bridge foundation is determined by the complex interaction of the water moving over the soil surrounding the foundation, this report utilized soil properties to estimate categories of soil erodibility. This allows engineers to apply less conservative assumptions for a subset of new bridge designs and reallocate limited resources that would have been spent on "overbuilding" this subset of bridges to other bridges that are most susceptible to scouring and would benefit from more conservative design assumptions. To incorporate information about soil properties into bridge design, this report developed two methods for predicting the critical shear stress and associated erodibility of soils. The first predicts critical shear stress using the Navarro/Hobson and Wang equations, and the second predicts the critical shear stress using USCS soil types with the purpose of placing the soils in erodibility categories.

Together, these two methods achieve complementary goals. The first method, which uses the Navarro/Hobson and Wang equations, is more accurate and produces a predicted shear stress value and associated soil erodibility category that can be used in design and assessment calculations. The second method predicts a range of critical shear stresses based on the USCS soil type or soil description, which is often one of the few pieces of information about soils that is recorded on boring logs. The second method also describes how water content information, if available, can be used to divide CL and CH clays into moderately resistant and resistant erodibility categories. Although the second method is less accurate, it allows engineers to use information contained on boring logs to estimate the soil's critical shear stress and associated erodibility category and identify those soils that are most susceptible to scour.

Information about soil properties can also support better allocation of funding for repair activities on existing bridges. The report determined which existing bridges are most vulnerable to scour using the FHWA risk-assessment tool called HYRISK. HYRISK was then modified to include a soil erodibility factor in the ranking of bridges. Finally, the ranked Georgia bridges were then re-ranked and compared to their original ranks after a downward soil erodibility adjustment factor was applied to the bridges.

Therefore, this report focused on several key methods to predict the critical shear stress of soils that do not necessarily involve returning a boring sample to a lab for critical shear stress tests. The goal of these methodologies is to provide a faster and more cost-effective approach to balance funding for new and existing bridges while simultaneously ensuring safe bridge foundations and minimizing economic consequences associated with overbuilding a bridge and/or having to retrofit or replace a bridge that has scour damage due to underbuilding it to withstand a major storm event.

Summary and Directions for Future Research

This project developed a methodology for including soil erodibility as an additional factor for assessing risk of bridge failure into HYRISK. The methodology used the USCS soil classification system as an initial evaluation of soil erodibility in terms of an erodibility category based on the critical shear stress of the soil. At this preliminary evaluation level, only field boring logs and assignments of USCS soil groups are required. For a higher level evaluation, the researchers' applied regression equations developed for the critical shear stress of fine and coarse-grained soils in Georgia based on field and laboratory

sample testing in an erosion flume in the laboratory. The initial evaluation, and the higher level evaluation, when more field data on soil properties were available, was applied to a sample of 38 bridges in Georgia which were then ranked according to risk of failure using HYRISK. Significant changes in rank were found to occur when the soil erodibility factor was included in the risk assessment. The initial evaluation proved to be a less refined evaluation of soil erodibility given its inherent lower field data requirements. As a result, less reduction in risk could be obtained from the soil erodibility evaluations. The higher level evaluation, on the other hand, provides a more realistic assessment of the influence of soil erodibility on risk and requires only soil grain size distribution and water content in order to be applied. Where possible it is recommended that the initial evaluation be applied first, and then the higher level assessment can be applied to the bridges with highest risk of failure by obtaining the additional field data required. In bridges with very large risks determined from the higher level evaluation, soil samples should be tested directly for erodibility in a flume designed for that purpose.

There are several limitations of this analysis. It is important to recognize that the analysis is based on Georgia soils and the underlying equations the authors used to relate soil properties to critical shear stress are state-specific. Thus, the relationships between critical shear stress and soil properties will likely differ across states, and Eqs. (2.7) and (2.9) should be calibrated using state-specific data before they are applied in other contexts. The comparison of HYRISK rankings based on the USCS classification versus the method that used the Navarro/Hobson and Wang equations is enlightening, as it shows "how much" can be gained from just using a simple USCS classification, as well as "how much more"

can be gained if more extensive soil property information. This raises an important direction for future research, namely whether it is possible to use other soil property characteristics (in addition to or instead of the USCS classification) to assign soil erodibility categories and corresponding K_2 risk adjustment factors for HYRISK. Ideally, these soil properties should be routinely found on boring logs or in a state's bridge asset management system, so that the risk adjustment factors can be calculated for a large proportion of the state's bridges. This paper has shown one way in which these adjustment factors can be calculated using the USCS classification; however, it may be viable to use other soil properties as well.

REFERENCES

1. Aberle, J., Nikora, V., McLean, S., Doscher, C., McEwan, I., Green, M., Goring, D., and Walsh, J. (2003). "Straight benthic flow-through flume for in situ measurement of cohesive sediment dynamics." *Journal of Hydraulic Engineering*, 129(1), 63–67.
2. Aberle, J., Nikora, V., and Walters, R. (2002). "In situ measurement of cohesive sediment dynamics with a straight benthic flume." *Hydraulic Measurements and Experimental Methods*, 1–10.
3. Aberle, J., Nikora, V., and Walters, R. (2004). "Effects of bed material properties on cohesive sediment erosion." *Marine Geology*, 207(1-4), 83–93.
4. Aberle, J., Nikora, V., and Walters, R. (2006). "Data interpretation for in situ measurements of cohesive sediment erosion." *Journal of Hydraulic Engineering*, 132(6), 581–588.
5. Adachi, T. and Ellingwood, B.R. (2010). "Comparative assessment of civil infrastructure network performance under probabilistic and scenario earthquakes." *Journal of Infrastructures Systems*, 16(1), 1-10.
6. Alhadeff, S.J., Musser, J.W., Sandercock, A.C., and D. T. R. (2000). *Digital Environmental Atlas of Georgia*: *Georgia Geologic Survey Publication CD1*, 2 CD-ROM set.
7. Allen, P. M., Arnold, J., and Jakubowski, E. (1999). "Prediction of stream channel erosion potential." *Journal of Environmental & Engineering Geoscience*, 5(3), 339–351.

8. Amos, C. L., Daborn, G., Christian, H. A., Atkinson, A., and Robertson, A. (1992a). "In situ erosion measurements on fine-grained sediments from the Bay of Fundy." *Marine Geology*, 108(2), 175–196.
9. Amos, C. L., Grant, J., Daborn, G.R. and Black, K. (1992b). "Sea Carousel - A benthic, annular flume." *Estuarine*, Coastal and Shelf Science, 34(6), 557–577.
10. Ansari, S., Kothyari, U., and Raju, K. (2003). "Influence of cohesion on scour under submerged circular vertical jets." *Journal of Hydraulic Engineering*, 129(12), 1014–1019.
11. Arneson, L. A., Zevenbergen, L. W., Lagasse, P. F., and Clopper, P. E. (2012). *Hydraulic Engineering Circular No. 18 (HEC-18): Evaluating Scour at Bridges*. Fifth Edition. Available at www.fhwa.dot.gov/engineering/hydraulics/pubs/hif12003.pdf.
12. ASTM International (American Society for Testing and Materials). (2005). "Standard test methods for liquid limit, plastic limit, and plasticity index of soils." D4318-05, ASTM International, West Conshohocken, PA.
13. ASTM International (American Society for Testing and Materials). (2011a). "Standard practice for classification of soils for engineering purposes (Unified Soil Classification System)." D2487-11, ASTM International, West Conshohocken, PA.
14. ASTM International (American Society for Testing and Materials). (2011b). "Standard practice for description and identification of soils (visual-manual procedure)," D2488-09a, ASTM International, West Conshohocken, PA.

15. Barry, K. M., Thieke, R. J., and Mehta, A. J. (2006). "Quasi-hydrodynamic lubrication effect of clay particles on sand grain erosion." *Estuarine, Coastal and Shelf Science*, 67(1), 161–169.

16. Briaud, J.-L., Ting, F., Chen, H., Cao, Y., Han, S., and Kwak, K. (2001). "Erosion function apparatus for scour rate predictions." *Journal of Geotechnical and Environmental Engineering*, 127(2), 105–113.

17. Briaud, J., Ting, F. Chen, H. Gudavalli, R., Perugu, S., and Wei, G. (1999). "SRICOS: Prediction of scour rate in cohesive soils at bridge piers." *Journal of Geotechnical and Environmental Engineering*, 125(4), 237–246.

18. Budhu, M. (2011). *Soil Mechanics and Foundations*, Third Edition. Hoboken, NJ: John Wiley and Sons.

19. CDC (Centers for Disease Control and Prevention). (1994). "Flood-related mortality - Georgia, July 4-14, 1994." *MMWR Weekly*, 43(29), 526-530. July 29, 1994. Available at http://www.cdc.gov/mmwr/preview/mmwrhtml/00032058.htm.

20. Charonko, C. M. (2010). *Evaluation of an In Situ Measurement Technique for Streambank Critical Shear Stress and Soil Erodibility.* M.S. Thesis, Biological Systems Engineering, Virginia Polytechnic Institute and State University.

21. Clopper, P. E., and Lagasse, P. F. (2011). Hydrologic uncertainty in prediction of bridge scour. *Transportation Research Record,* 2262, 207–213.

22. Cook, R., Garner, M.K., Morris, M. and Matteucci, M. (2009). "Flood death toll at 9." *Atlanta Journal Constitution*, Atlanta. September 26, 2009. Available at http://www.ajc.com/news/news/local/flood-death-toll-at-9/nQTNr/.

23. Debnath, K., Nikora, V., Aberle, J., Westrich, B., and Muste, M. (2007a). “Erosion of cohesive sediments: Resuspension, bed load, and erosion patterns from field experiments.” *Journal of Hydraulic Engineering*, 133(5), 508–520.

24. Debnath, K., Nikora, V., and Elliott, A. (2007b). “Stream bank erosion: In situ flume tests.” *Journal of Irrigation and Drainage Engineering*, 133(3), 256–264.

25. Ellingwood, B. R. (2000). “LRFD: Implementing structural reliability in professional practice.” *Engineering Structures*, 22, 106-115.

26. Ganaoui, O., Schaaff, E., Boyer, P., Amielh, M., Anselmet, F., and Grenz, C. (2007). “Erosion of the upper layer of cohesive sediments : Characterization of some properties.” Journal of Hydraulic Engineering, 133(9), 1087–1091.

27. Ghosn, M. (2005). “Load combination factors for extreme events.” Transportation Research Record, Issue CD 11-S, 389-397.

28. Gotvald, A.J., and McCallum, B. E. (2010). “Epic flooding in Georgia, 2009.” *USGS*, 1-2. Available at http://pubs.usgs.gov/fs/2010/3107/pdf/fs2010-3107.pdf.

29. Grabowski, R.C., Droppo, I.G. and Wharton, G. (2011). “Erodibility of cohesive sediment: The importance of sediment properties.” *Earth-Science Reviews*, 3/4, 101-120.

30. Gust, G., and Morris, M. J. (1989). “Erosion thresholds and entrainment rates of undisturbed in situ sediments.” *Journal of Coastal Research*, Special Issue No. 5, 87–99.

31. Hansen, G. J. (1991). “Development of a jet index to characterize erosion resistance of soils in earthen spillways.” *Transactions of the ASAE*, 34(5): 2015-2020.

32. Hanson, G. J., and Simon, A. (2001). "Erodibility of cohesive streambeds in the loess area of the midwestern USA." *Hydrological Processes*, 15, 23–38.

33. Hanson, G.J., Cook, K. R. (2004). "Apparatus, test procedures, and analytical methods to measure soil erodibility in situ." *Applied Engineering in Agriculture*, 20(4), 455–462.

34. Hobson, P. M. (2008). *Rheologic and Flume Erosion Characteristics of Georgia Sediments from Bridge Foundations*. M.S. Thesis, Civil and Environmental Engineering, Georgia Institute of Technology, Atlanta, GA.

35. Hobson, P., Navarro, H. and Sturm, T.W. (2010). "Erodibility of sediment at bridge foundations in Georgia." Paper presented at the 2nd Joint Federal Interagency Conference, Las Vegas, Nevada. 7 pp. Available at http://acwi.gov/sos/pubs/2ndJFIC/Contents/5A4%20Sturm_3_10_2010_paper.pdf.

36. Holtz, R. D. and Kovacs, W. D. (1981). Introduction to Geotechnical Engineering. Englewood Cliffs, N.J. : Prentice-Hall

37. Houwing, E.-J., and van Rijn, L. C. (1998). "In Situ Erosion Flume (ISEF): determination of bed-shear stress and erosion of a kaolinite bed." *Journal of Sea Research*, 39(3-4), 243–253.

38. IPCC (Intergovernmental Panel on Climate Change). (2007). *Climate Change 2007: Synthesis Report*. Contribution of Working Groups I, II and III to the Fourth Assessment Report of the Intergovernmental Panel on Climate Change [Core Writing Team, Pachauri, R.K and Reisinger, A. (eds.)]. IPCC, Geneva, Switzerland, 104 pp.

39. Ivey, L. M., Rix, G. J., Werner, S. D., and Erera, A. L. (2010). "A framework for earthquake risk assessment for container ports." *Paper presented at the 89th Annual Meeting of the Transportation Research Board:* Washington, DC.

40. Jacobs, W., Le Hir, P., Van Kesteren, W., and Cann, P. (2011). Erosion threshold of sand-mud mixtures. *Continental Shelf Research*, 31, S14-S25.

41. Johnson, P. A. (1995). "Comparison of pier-scour equations using field data." *Journal of Hydraulic Engineering*, 121(8), 626-629.

42. Johnson, P. A. (1996). "Uncertainty of hydraulic parameters." *Journal of Hydraulic Engineering*, 122(2), 112–114.

43. Johnson, P. A., and Niezgoda, S. L. (2004). "Risk-based method for selecting bridge scour countermeasures." *Journal of Hydraulic Engineering*, 130(2), 121–128.

44. Khelifa, A., Garrow, L. A., Higgins, M. J., and Meyer, M. D. (2013). "Impacts of climate change on scour-vulnerable bridges: Assessment based on HYRISK." *Journal of Infrastructure Systems*, 19(2), 138–146.

45. Krishnappan, B. G. (2007). "Recent advances in basic and applied research in cohesive sediment transport in aquatic systems." *Canadian Journal of Civil Engineering*, 34(6), 731–743.

46. Maa, J. P.-Y., Wright, L. D., Lee, C.-H., and Shannon, T. W. (1993). "VIMS Sea Carousel: A field instrument for studying sediment transport." *Marine Geology*, 115(3-4), 271–287.

47. Mallison, T. L. (2008). *Comparing In Situ Submerged Jet Test Device and Laboratory Flume Methods to Estimate Erosional Properties of Cohesive Soils for Bank Stability Models.* M.S. Thesis, Environmental Engineering, The University of Tennessee, Knoxville, TN.

48. Mazurek, K., Rajaratnam, N., and Sego, D. (2001). "Scour of cohesive soil by submerged circular turbulent impinging jets." *Journal of Hydraulic Engineering*, 127(7), 598–606.

49. McNeil, J., Taylor, C., and Lick, W. (1996). "Measurements of erosion of undisturbed bottom sediment with depth." *Journal of Hydraulic Engineering*, 122(6), 316–324.

50. Mehta, A. J. (1991). *Characterization of Cohesive Soil Bed Surface Erosion, with Special References to the Relationship between Erosion Shear Strength and Bed Density*. M.S. Thesis, Coastal and Oceanographic Engineering Department, University of Florida, Gainsville, FL.

51. Milley, P. C. D., Betancourt, J., Falkenmark, M., Hirsch, R. M., Kundzewicz, Z. W., Lettenmaier, D. P., and Stouffer, R. J. (2008). "Stationarity is dead: Whither water management?" *Science Magazine*, 319(1), 573–574. Available at http://wwwpaztcn.wr.usgs.gov/julio_pdf/milly_et_al.pdf.

52. Navarro, H. R. (2004). *Flume Measurements of Erosion Characteristics of Soils at Bridge Foundations in Georgia*. M.S. Thesis, Civil and Environmental Engineering, Georgia Institute of Technology, Atlanta, GA.

53. Niezgoda, S. L., and Johnson, P. A. (2007). “Case study in cost-based risk assessment for selecting a stream restoration design method for a channel relocation project.” *Journal of Hydraulic Engineering*, 133(5), 468–481.

54. Niezgoda, S. L., and Johnson, P. A. (2012). “Applying risk-benefit analysis to select an appropriate streambank stabilization measure.” *Journal of Hydraulic Engineering*, 138(5), 449–461.

55. NRC (National Research Council). (2009). *Informing Decisions in a Changing Climate*. Panel on Strategies and Methods for Climate-related Decision Support, Committee on the Human Dimensions of Global Change. Division of Behavioral and Social Sciences and Education. Washington, DC: The National Academies Press.

56. Partheniades, (2010). *Cohesive sediments in open channels: Properties, transport and applications,* Elsevier, New York.

57. Paterson, D. M. (1989). “Short-term changes in the erodibility changes of intertidal cohesive sediments related to the migratory behavior of epipelic diatoms.” *Limnology and Oceanography*, 34(1), 223–234.

58. Potter, K.N., Velazquez-Garcia, J. de J., and Torbert, H. A. (2002). “Use of a submerged jet device to determine channel erodibility coefficients of selected soils of Mexico.” *Journal of Soil and Water Conservation*, 57(5), 272–277.

59. Ravens, T. M. (2007). “Comparison of two techniques to measure sediment erodibility in the Fox River, Wisconsin.” *Journal of Hydraulic Engineering*, 133(1), 111–115.

60. Ravens, T. M., and Gschwend, P. M. (1999). “Flume measurements of sediment erodibility in Boston Harbor.” *Journal of Hydraulic Engineering*, 125(10), 998–1005.

61. Ravisangar, V., Dennett, K., Sturm, T., and Amirtharajah, A. (2001). “Effect of sediment pH on resuspension of kaolinite sediments.” *Journal of Environmental Engineering*, 127(6), 531–538.

62. Ravisangar, V., Sturm, T.W., and Amirtharajah, A. (2005). “Influence of sediment structure on erosional strength and density of kaolinite sediment beds.” *Journal of Hydraulic Engineering*, 131(5), 356-365.

63. Roberts, J., Jepsen, R., Gotthard, D., and Lick, W. (1998). "Effects of particle size and bulk density on erosion of quartz particles." *Journal of Hydraulic Engineering*, 124(12), 1261-1267.

64. Roberts, J., Jepsen, R., and James, S. (2003). “Measurements of sediment erosion and transport with the adjustable shear stress erosion and transport flume.” *Journal of Hydraulic Engineering*, 129(11), 862–871.

65. Schmidt, N. (2008). *Climate Change and Transportation: Challenges and Opportunities.* M.S. Thesis, Civil and Environmental Engineering, Georgia Institute of Technology, Atlanta, GA.

66. Schünemann, M., and Kühl, H. (1993). “Experimental investigations of the erosional behavior of naturally formed mud from the Elbe Estuary and adjacent Wadden Sea, Germany.” In *Nearshore and Estuarine Cohesive Sediment Transport, Coastal and Estuarine Studies*, (A. J. Mehta, ed.). Washington, DC: American Geophysical Union, 314–330.

67. Stein, S. M., Young, G. K., Pearson, D. R., and Trent, R. E. (1999). "Prioritizing scour vulnerable bridges using risk." *Journal of Infrastructure Systems*, 5(3), 95–101.

68. Stein, S., and Sedmera, K. (2006). *Risk-Based Management Guidelines for Scour at Bridges with Unknown Foundations*. TRB's National Cooperative Highway Research Program (NCHRP) Web-Only Document 107. Available at http://onlinepubs.trb.org/onlinepubs/nchrp/nchrp_w107.pdf.

69. Sturm, T. W., Hong, S. H., and Hobson, P. (2008). Estimating critical shear stress of bed sediment for improved prediction of bridge contraction scour in Georgia. Georgia DOT, *Report No. FHWA-GA-08-0617*, Atlanta, GA.

70. Sturm, T. W. (2010). *Open Channel Hydraulics*. New York: McGraw Hill.

71. Thoman, R. and Niezgoda, S. (2008). "Determining erodibility, critical shear stress, and allowable discharge estimates for cohesive channels: Case study in the Powder River Basin of Wyoming." *Journal of Hydraulic Engineering*, 134(12), 1677–1687.

72. Ting, F., Briaud, J., Chen, H., Gudavalli, R., Perugu, S., and Wei, G. (2001). "Flume tests for scour in clay at circular piers." *Journal of Hydraulic Engineering*, 127(11), 969–978.

73. Tolhurst, T., Black, K., and Paterson, D. (2009). "Muddy sediment erosion: Insights from field studies." *Journal of Hydraulic Engineering*, 135(2), 73–78.

74. Tolhurst, T. J., Black, K. S., Shaylerb, S. A., Mathera, S., Black, I., Baker, K., and Patersona, D. M. (1999). "Measuring the in situ erosion shear stress of intertidal sediments with the cohesive strength meter (CSM)." *Estuarine, Coastal and Shelf Science*, 49(2), 281–294.

75. Tsai, C.-H., and Lick, W. (1986). “A portable device for measuring sediment resuspension.” *Journal of Great Lakes Research*, 12(4), 314–321.

76. U.S. DOT (U.S. Department of Transportation). (2006). *U.S. Department of Transportation Strategic Plan 2006-2011*. Washington, DC.

77. Wang, Y.-C. (2013). *Effects of Physical Properties and Rheological Characteristics on Critical Shear Stress of Fine Sediments*. Ph.D. Thesis, Civil and Environmental Engineering, Georgia Institute of Technology, Atlanta, GA.

78. Watts, C. W., Tolhurst, T. J., Black, K. S., and Whitmore, A. P. (2003). “In situ measurements of erosion shear stress and geotechnical shear strength of the intertidal sediments of the experimental managed realignment scheme at Tollesbury, Essex, UK.” *Estuarine, Coastal and Shelf Science*, 58(3), 611–620.

79. Williamson, H. J., and Ockenden, M. C. (1996). “ISIS : An instrument for measuring erosion shear stress in situ.” *Estuarine, Coastal and Shelf Science*, 42(1), 1–18.

80. Witt, O., and Westrich, B. (2003). “Quantification of erosion rates for undisturbed contaminated cohesive sediment cores by image analysis.” *Hydrobiologia*, 494(1-3), 271–276.

81. Wynn, T., and Mostaghimi, S. (2006). “The effects of vegetation and soil type on streambank erosion, southwestern Virginia, USA.” *Journal of the American Water Resources Association*, 42(1), 69–82.

82. Young, R. A. (1977). “Seaflume: A device for in-situ studies of threshold erosion velocity and erosional behavior of undisturbed marine muds.” *Marine Geology*, 23(1-2), 11–18.

83. Zreik, D., Krisnappan, B., Germaine, J., Madsen, O., and Ladd, C. (1998). “Erosional and mechanical strengths of deposited cohesive sediments.” *Journal of Hydraulic Engineering*, 124(11), 1076–1085.